STUDIES ON PARAMAGNETIC AND REDOX PROPERTIES OF SOME METALLOPORPHYRINS

Thesis submitted in fulfillment of the

requirements for the degree of

Doctor of Philosophy

By

A. Murugan

DEPARTMENT OF CHEMISTRY

SCHOOL OF PHYSICAL SCIENCES

NORTH EASTERN HILL UNIVERSITY

SHILLONG - 793 022

April - 2008

Declaration

North-Eastern Hill University
Shillong-793 022
April 2008

I, **A.Murugan**, hereby declare that the subject matter of this thesis is the record of work done by me, that the contents of this thesis did not form basis of the award of any previous degree to me or to the best of my knowledge to anybody else, and that the thesis has not been submitted by me for research degree in any other University/Institute.

This is being submitted to the North-Eastern Hill University for the **Ph.D** Degree in **Chemistry.**

(A. Murugan)
CANDIDATE

(Dr. Aka Lemtur)
SUPERVISOR

Reader
Department of Chemistry
North-Eastern Hill University
Shillong- 793022

(Prof. R. H. Duncan Lyngdoh)
HEAD
DEPARTMENT OF CHEMISTRY,
NORTH-EASTERN HILL UNIVERSITY
SHILLONG.

Head
Department of Chemistry
North-Eastern Hill University
Shillong- 793022.

Dr. A. Lemtur
Department of Chemistry
North Eastern Hill University
Shillong 793022

email:lemtur1@rediffmail.com
tel. no. 0364 272 2618
fax no: 0364 2550076

CERTIFICATE

This is to certify that the thesis entitled "Studies on paramagnetic and redox properties of some metalloporphyrins" is based on the original work done by A. Murugan, under my supervision in the Department of Chemistry, School of Physical Sciences, North Eastern Hill University, Shillong Meghalaya. This work has not previously formed the basis for the award of any degree, diploma, associateship, fellowship or any other similar title and that it represents entirely an independent work on the part of the candidate.

Prof. R. H. Duncan Lyngdoh
Head
Department of Chemistry

Head
Department of Chemistry
North-Eastern Hill University
Shillong-793022.

Dr. AKa Lemtur
Supervisor

Reader
Department of Chemistry
North-Eastern Hill University
Shillong-793022

Place: Shillong

Date: 29.04.2008

ACKNOWLEDGMENTS

I am extremely grateful and deeply indebted to my supervisor **Dr. Aka Lemtur**, Reader, Department of Chemistry, NEHU,Shillong for his stimulating guidance, constant encouragement and untiring help throughout the course of the study.

I would like to thank the Head, Department of Chemistry, **Prof. R. H. Duncan Lyngdoh,** NEHU, Shillong for all the help rendered to me.

It is with great pleasure; I record my gratitude to **Prof. K. Ismail**, Dean, School of Physical Science, NEHU, and Shillong for his constant help and encouragement throughout the course of this work.

I have immense pleasure in recording my profound sense of gratitude to **Prof. R. K. Poddar,** Department of Chemistry, NEHU, Shillong for his constructive suggestions during every stage of my research work. My thanks go to the Department of Chemistry, NEHU, Shillong, for all the facilities available and to all the faculty members for their gracious encouragement.

I am also thankful to **Prof. N. Venugopal**, Department of Botany, NEHU,and **Mr. Isias**, Teacher, St'Mary Hr.Sec.School, Shillong for their inspiration and untiring help during my stay at Shillong.

I thank my senior and labmate **Dr. A. Tomba Singh, Dr(Mrs) Cornelia Mr. Donborlang, Mrs. Aicydalyne Snaitang** for their help and moral support.

I owe my sincere thanks to **Prof. J. Subramanian**, NMR Section, CLRI, Chennai, **Prof. P. Sambasiva Rao, Mr. B. Natarajan,** Department of Chemistry, Pondicheery Universiy, Pondicheery, **Dr. V. Manivannan**, Department of Chemistrh,IITGuwahati and **Mr. Sivaramakrishnan**, SAIF, IIT Madras , Chennai for their help in the EPR measurement. I am also thankful to **Prof. P. R. Athappan and Mr. Prabakaran** , Department of Inorganic Chemistry,. Madurai Kamaraj University, Madurai for their help in the CV measurements.

I express my sincere thanks to the **Prof. O. K.Medhi,** Department of Chemistry, Gauwahati University, Guwahati for his keen interest in my work.

I would like to express my thanks to **Mrs. Florence** for recording the UV spectra. My sincere gratitude goes to **Mr. Thomas** and other office staff for their help, rendered to me during the course of my Ph.D work.

I owe my sincere thanks to **Dr. Kiranmay Sarma**, Faculty USEM Guru Gobind Sing Indraprastha University, Kashmere Gate, New Nelhi, **Dr. Om Prakash Tripathi,** Lecturer in Forsty Department, NERST, Arunachal Pradesh, **Dr. Krishna Upadya**, Faculty in NEHU, Shillong, **Dr. Bidyadhar Das** for their support, help and inspiration.

Thanks are also due to my friends, **Dr. S. Jeeva, Dr. A. Murugesan, Dr. Senthikumar,, Dr. P. Sudhakar, Mr. P. RajKumar, Dr. A. Shankaran, Mr. Kathirvel , Mr. K. Dharmaraj, Mr.C.Kadakkarai, Mr. Mithun Chakrabarty, Miss. Snigdha Chanda, Miss. Juthika Das, Miss. Dipannita Das, Mr. Johar Dey, Mr. Joseph Jeremiah, Mr. Haans J.Freddy, Mr. Allen J.Freddy,** and **Mr. N. Ambikapathy** who have helped in various aspects during the course of the my research workI express my sincere gratitude to my beloved Parents and brothers for their co-operation, encouragement and inspiration for completing this research work successfully.

“My help cometh from the Lord which made heaven and earth”. Lastly I express my gratitude to God Almighty without whom I would have not been able to complete this research work. I also dedicate this work to Him.

A.Murugan

Contents

Page No

List of Tables (i)

List of Figures (ii)

Preface 1

Introduction 3

References 4

Chapter 1. A brief review of the EPR and cyclic voltammetric studies of some vanadyl porphyrins 7

References 11

Chapter 2. Experimental Section

2.1. Introduction 13

2.2 Solvents 13

2.3. Oxidizing agent 14

2.4 Reagents and supporting electrolytes 14

2.5 Synthesis of porphyrins 15

2.6. Synthesis of metalloporphyrins 18

2.7 Instrumentation 21

References 23

Chapter 3. Cyclic voltammetric studies of some metalloporphyrins

3.1. Introduction 24

3.2. Principle of cyclic voltammetry 30

3.3. Experimental details 34

3.4. Results and discussion 34

3.5. Conclusion 40

References 46

Chapter 4. Cyclic voltammetric studies of some manganese, cadmium and copper porphyrins

4.1. Introduction 48
4.2. Results of manganese porphyrins 48
4.3. Discussion of manganese porphyrins 50
4.4. Conclusion of manganese porphyrins 51
4.5. Results of cadmium and copper porphyrins 52
4.6 discussions of cadmium and copper porphyrins 53
4.7. Conclusion of cadmium and copper porphyrins 53
References 69

Chapter 5. EPR of some substituted vanadyl meso-tetraphenyl porphyrins oxidized with $SbCl_5$

5.1. Introduction 71
5.2. Some basic principles of EPR 72
5.2.1. Resonance condition, g-value and symmetry 72
5.2.3. Zerofield splitting and fine structure 75
5.3. Hyperfine interaction 77
5.4. Line shape and relaxation 78
5.5. Spin Hamiltonian 80
5.6. Metalloporphyrins with paramagnetic metal atom unpaired electron on the ligand 81
5.7. EPR of some substituted vanadyl mesotetraphenyl porphyrins oxidized with $SbCl_5$ 83
5.7.1. Results 83
5.7.2 Discussion 84
5.7.3. Conclusion 85
References 96
Appendix A 99

LIST OF TABLES

Page No.

Table:3.1 Cyclic voltammetric data for vanadyl porphyrins at room Temperature 41

Table:4.1 Cyclic voltammetric data for manganese porphyrins at room temperature 55

Table:4.2 Cyclic voltammetric data for Cadmium and Copper porphyrins at room 64

Table.5.1: ESR spectrum at Room Temperature 86

LIST OF FIGURES

Page No

Figure.3.1.1a. Structure of free porphyrin and metalloporphyrin 25

Figure.3.1.1b. Structure of free porphyrin and metalloporphyrin 26

Figure.3.1.2. HOMO representation for metalloporphyrins 28

Figure.3.2.1. Electrochemical cell for quality cyclic voltammetry experiment.31

Figure.3.2.2. Triangular wave 32

Figure.3.4.1. Cyclic voltammogram of VO[T(2,5-$(OCH_3)_2$)PP] in CH_2Cl_2 Containing 0.1M TBAP at room temperature 42

Figure.3.4.2. Cyclic voltammogram of VO[T(*p*-OH)PP] in CH_2Cl_2 Containing 0.1M TBAP at room temperature 43

Figure.3.4.3. Cyclic voltammogram of VO[T(*o*-NO_2)PP] in CH_2Cl_2 Containing 0.1M TBAP at room temperature 44

Figure.3.4.4. Cyclic voltammogram of VO[T*py*P] in CH_2Cl_2 Containing 0.1M TBAP at room temperature 45

Figure.4.2.1. Cyclic voltammogram of Mn[T(2,5-$(OCH_3)_2$)PP] in CH_2Cl_2 Containing 0.1M TBAP at room temperature 56

Figure.4.2.2 .Cyclic voltammogram of Mn[T(*p*-OH)PP] in CH_2Cl_2 Containing 0.1M TBAP at room temperature 57

Figure.4.2.3 Cyclic voltammogram of Mn[T(*o*-NO_2)PP] in CH_2Cl_2 Containing 0.1M TBAP at room temperature 58

Figure.4.2.4. Cyclic voltammogram of Mn[T*py*P] in CH_2Cl_2 Containing 0.1M TBAP at room temperature 59

Figure.4.3.1.. UV-visible absorption spectrum of Mn[T(2,5-$(OCH_3)_2$)PP] in CH_2Cl_2 oxidized with (———) $SbCl_5$ at room temperature, (------) and (-------) reduced with diethyl amine 60

Figure.4.3.2.. UV-visible absorption spectrum of Mn[T(p-OH)PP]in CH_2Cl_2 ~~oxidized~~ with (———) $SbCl_5$ at room temperature, (--------), and (----) reduced with diethyl amine 61

Figure.4.3.3.. UV-visible absorption spectrum of Mn[T(*o*-NO_2)PP] in CH_2Cl_2 ~~oxidized~~ with (———) $SbCl_5$ at room temperature, (---------) and (----) reduced with diethyl amine 62

Figure.4.3.4. UV-visible absorption spectrum of Mn[TpyP] in CH_2Cl_2 oxidized with(———)$SbCl_5$ at room temperature, (---------), and (----) reduced with diethyl amine 63

Figure.4.5.1 .Cyclic voltammogram of Cd[T(2,5-$(OCH_3)_2$)PP] in CH_2Cl_2 Containing 0.1M TBAP at room temperature 65

Figure.4.5.2. Cyclic voltammogram of Cd[T(*o*-NO_2)PP] in CH_2Cl_2 Containing 0.1M TBAP at room temperature 66

Figure.4.5.3. Cyclic voltammogram of Cu[T(2,5-$(OCH_3)_2$)PP] in CH_2Cl_2 Containing 0.1M TBAP at room temperature 67

Figure.4.5.4. Cyclic voltammogram of Cu[T(*o*-NO_2)PP] in CH_2Cl_2 Containing 0.1M TBAP at room temperature 68

Figure.5.2.1. Effect of Zero field splitting, Energy levels (i)A Triplet state (ii) A quartet state for of an axially symmetric system 76

Figure.5.7.1 (i).X-band EPR spectra of $VO[T(o\text{-}NO_2)PP]$ in CH_2Cl_2 oxidized with $SbCl_5$ at room temperature 87

Figure.5.7.1 (ii) A and B.X-band EPR spectra of $VO[T(2,5\text{-}(OCH_3)_2)PP]$ in CH_2Cl_2 oxidized with $SbCl_5$ at room temperature 88

Figure.5.7.1 (iii) A and B.X-band EPR spectra of VO[TpyP] in CH_2Cl_2 Oxidized with $SbCl_5$ at room temperature 89

Figure.5.7.1 (iv). A,B and C.X-band EPR spectra of VO[T(p-OH)PP]in CH_2Cl_2 oxidized with $SbCl_5$ at room temperature 90

Figure.5.7.1. (v).Infrared spectra of $VO[T(2,5\text{-}(OCH_3)_2)PP]$ in CH_2Cl_2 Oxidized with $SbCl_5$ at room temperature 91

Figure.5.7.1 (vi) A..UV-visible absorption spectrum of $VO[T(2,5\text{-}(OCH_3)_2)PP]$ in CH_2Cl_2 oxidized with(____) $SbCl_5$ at room temperature, (….) and (------) reduced with diethyl amine 92

Figure.5.7.1 (vi) B..UV-visible absorption spectrum of VO[T(p-OH)PP]in CH_2Cl_2 oxidized with(_____)$SbCl_5$ at room temperature, (------),and (-------) reduced with diethyl amine 93

Figure.5.7.1 (vi) C..UV-visible absorption spectrum of $VO[T(o\text{-}NO_2)PP]$ in CH_2Cl_2 oxidized with(——)$SbCl_5$ at room temperature, (-------),and (-------) reduced with diethyl amine 94

Figure.5.7.1 (vi) D..UV-visible absorption spectrum of VO[TpyP] in CH_2Cl_2 oxidized with(——)$SbCl_5$ at room temperature, (-------), and (--------) reduced with diethyl amine 95

Preface

Porphyrin chemistry is an old chemistry and is an area which is researched widely, in spite of the voluminous information available. New porphyrins are synthesized and more new results appear in the literature everyday. This is because porphyrins are not only biologically important but also find their way in the field of medicine and material sciences. Quite a good number of modified and new porphyrin ligands are available in the literature. But metal complexes of such porphyrins are not properly explored. This provides us an opportunity to venture into this field of research. This thesis embodies the physico-chemical studies of some vanadyl porphyrins and manganese porphyrins which are not reported so far in the literature.

This thesis consists of five chapters. Chapter 1 presents a brief review of the EPR and Cyclic voltammetric studies of some vanadyl porphyrins.

Chapter 2 describes different experimental techniques and measurements used in the course of the investigation.

Chapter 3 presents cyclic voltammetric studies of some vanadyl porphyrins.

Chapter 4 deals with cyclic voltammetric studies of some manganese, cadmium and copper porphyrins.

Chapter 5 describes EPR of some substituted vanadyl meso-tetraphenyl porphyrins oxidized with $SbCl_5$

INTRODUCTION

Metalloporphyrins are not only biologically important class of compounds but find their applications in the field of medicine and material sciences[1,2]. Some metalloporphyrins are also used as catalyses[3] in the oxidation of alkenes. Vanadyl porphyrins are also found in the oil shells[4], which are believed to be of biological origin and provide valuable molecular fossil record of the past environmental conditions of the geological era. Synthetic porphyrins such as supra molecular porphyrin arrays provide nano scale optical and magnetic materials[5-12]. Such self assembled materials provide the possibilities in the formation of molecular electronic devices. Metalloporphyrin macro cycles are known as molecular building blocks of one –dimensional molecular metals[7].

It is well known that metalloporphyrin π-cation radicals exhibit similar properties with that of *chlorophyll a* and B_{chl}[14-20]. Occurrence of Fe(II)porphyrins π-cation radicals in cytochromes and heme catabolism are well documented[21,22]. It is also known that the oxidation of Fe(III)P occur in catalase and peroxidase[23].

Obviously, study of redox properties of metalloporphyrins will give some interesting information. The redox behavior of metalloporphyrins also depends on substituents in the ring.

REFERENCES

1. A.J.Crowe, *Tin and its uses*, **162**, 4(1990)

2. A.J.Crowe, *Tin and its uses*, **163**, 4(1990)

3. C,-J.Linu, W.-Y.Yu, S.-M.Peng, T.C.W.Mak, C,.M.Che, *J.Chem.Soc.Dalton trans.* **11**, 1805(1998)

4. J.A.Shelmutt and M.M.Dobry, *J.Phys.Chem.*, **87**(16) 3001(1988)

5. A.Osuka, M.Ikada, H.Sheratori, Y.Nishimura and I.Yamazuki, *J.Chem.Soc., Perkin trans.***2**,1019(1999)

6. K.Chichak and N.R.Branda, *Chem.Commun.*, 523(1999)

7. A.Rosa, E.J. Baerends , *Inorg.Chem.*,**32**,5637(1993)

8. K.Chichak and N.R.Branda, *Chem.Commun.*, 1211(2000)

9. T,-B.Tsao, G,-H, Lee, C.-Y.Yeh and S,-M.Peng, *Dalton trans.*, 1465(2003)

10. C.M.Drain, J.D.Batteas, G.W.Flynn, T.Millik, N.Chi, D.G.Yaslon and H.Sommers, Colloquin of Nat.ac.Scie "*Nanoscience :underlying physical concepts and phenomena*" Washington DC, May 18-20(2000), PNAS early edition

11. T.E.O.Sereen, K.B.Lawton, N.Dolney, R.Ispasolu, T.Goodson III, S.J.Martin, D.D.C.Bradley, H.LAnderson, *J.Mater, Chem.*, **11,**312(2001)

12. D.Kim and A.Osuka, *Acc.Chem.Res.*, **32(10),**375(2004)

13. R.Harada, H.Okawa, T.Kojima, *Inorg.Chim.Acta.*, **358**, 489(2005)

14. D.H.Kohl, in" *Biological applications of Electron Spin Resonance*", H.M.Wartz, J.R.Bolton and D.C.Borg.Ed., Wiley-Interscience, New York, N.Y., 1972, p213.

15. J.D.McElory, .Fehar, and D.Mauzerall, *Biochem.Biophys.Acta*, **267**, 363(1972)

16. W.W.Passon, *Biochem.Biophys.Acta*, **153**,248(1968)

17. P.A.Loach and K.Walsh, *Biochemistry*, **8,** 1908(1969)

18. J.R.Bolton, .E.Clayton and D.W.Reed, *Phot.Chem.Photbiol.*,**9**, 209(1969)

19. J.T.Warden and J.R.Bolton, *J.Am.Chem.Soc.*, **94**, 4351(1972)

20. D.Dolphin and R.H.Felton, *Acc.Chem.Res.* **7,** 26(1974)

21. C.E.Castro, *J.Theor.Biolo.*, **33**,475(1972)

22. (a) N.Sutin, and A.Forman, *J.Am.Chem.Soc.*, **93**,5274(1971)

(b) N.Sutin, *Chem.Brit.*, **8**. 148(1972)

23. C.A.Reed, in “*Electrochemical and spectrochemical studies of Biological Rex components*”, Advances in Chemistry series, Edited by K.M.Kadish (American chemical society, Washington.D.C., 1982), 201, p333.

Chapter 1

A brief review of the EPR and cyclic voltammetric studies of some vanadyl porphyrins

This chapter presents a brief review on vanadyl porphyrins of substituted TPP systems mainly focusing on the electron paramagnetic resonance (EPR) and Cyclic voltammetric (CV). studies

1.1.Vanadyl porphyrin

The EPR of the oxidation of VOTPP (Vanadyl tetraphenyl porphyrin) with $Br_2/SbCl_5/TiCl_4$ are available in the literature[1]. The biradical/triplet state generated by $SbCl_5$ could not be observed by earlier workers even in the glass state. Even the preoxidised complexes could be observed only at low temperatures. The reason for not observing these complexes was attributed to thermodynamic instability of these complexes at room temperature. Observation of smaller hyperfine coupling constant (at low temperature) was attributed to the compression N-V-N bonding due to the additional bonding of $[SbCl_4]^+$ or $[TiCl_3]^+$ or Cl^- with the oxygen of vanadyl. Hoshimo et al[2] could observe the triplet state at 77K. They have generated the triplet state by γ-irradiation. But they also could not observe $\Delta M_s = \pm 1$ transition which they attributed to the intense background signal of VOTPP.

They have estimated that vanadium atom to be 0.5A° out of plane of porphyrin plane. They also have suggested that $VOTPP^{+\cdot}$ to be in $^2A_{2u}$ state.

Later on Tomba[3] et al have reported the EPR of VOTPP oxidised with $SbCl_5$. They could observe the pre-oxidized species at room temperature. Even the triplet state could be observed at room temperature at higher modulation although the signal was quite broad. The formation of mono cation was further supplemented by IR spectra[4,5]. Further, formation of dication was also observed. On the basis of EPR data they have suggested the possibilities that some species with electron spin density in a_{1u} state co-exist. They also have reported the EPR of VO[T(*m*-NO_2)PP], VOTPP(Xn) (Xn =Br , n= 1 to 4), VO[T(*p*-X)PP] where X = Cl, Br, F, -CH_3 and –OCH_3[6]. The EPR spectra of the oxidation products of these compounds with $SbCl_5$ exhibit similar pattern to that of the oxidation products of VOTPP. Formations of cations are also supported by IR spectra. No significant changes in the EPR spectra were formed due to peripheral substitution. The average inter electron distance of 3.623±0.030A° is also reported. It has been suggested that some considerable unpaired π-electron density does exist in a_{1u} state although more dominantly in a_{2u} state.

On the other hand cyclic voltammetric studies have shown some considerable change in the oxidation potentials. Electrophilic substitutions in the exo-positions of the pyrrole ring shift the oxidation potentials to higher side. Substitution in the phenyl ring with electron withdrawing group shift the oxidation potentials to higher side, while substitution with electron donating group in the phenyl ring lowers the oxidation potentials.

Normally, metal $d_{xy}/d_{x^2-y^2}$-porphyrin (a_{1u})/(a_{2u}) interaction do not occur in a planar porphyrin complexes. This is because the metal d-orbitals are orthogonal to porphyrin ligand a_{1u}/a_{2u} HOMOS. Walker and Co-workers[7] have reported that d orbitals of the metal and a_{1u}/a_{2u} orbitals of porphyrin ligand can have interactions in ruffle and saddle distortions. Similar view is reported by Gosh et al[8], existence of such interactions is reported by Harada et al[9] in vanadyl complexes of octaphenyl porphyrin (VO(OPP)) and vanadyl dodecaphenyl porphyrin (VO(DPP)). They have observed that porphyrin with saddle distortion undergoes disproportionation on oxidation. This is due to destabilization of a_{1u} leading to accidentally degenerated with a_{2u}. Thus, a_{1u} type cation radical is unstable and disproportionate to dication and neutral species. Thus, HOMO-LUMO gap narrowing down is observed in the voltammogram. They further pointed out that in vanadyl porphyrins (VO(DPP)) (vanadyl dodecaphenyl porphyrin) due to ligand distortion a_{1u} orbital elevate leading to the narrowing of HOMO-LUMO gap. This narrowing is observed in lowering of the oxidation potentials in the voltammogram.

REFERENCES

1. G.E.Selyutin, A.A.Shklyaev and V.F.Anufrieko, *Dokl.Akad.Nauk.SSR,* **255**,390(1980)

2. M.Hoshino, S.Konishi, M.Imamura, S.Watanabe and Y.Hama, *Chem.Phys.Lett,* **102**,259(1983)

3. A.Tomba Singh and A.Lemtur, *Spectrochim,.Acta Part* A, **59**, 1549(2003)

4 E.T.Shimomura, M.A.Phillippi, H.M.Goff, W.F.Schulz and C.A.Reed, *J.Am.Chem.Soc.***103,** 6778(1981)

5 A.S.Hinman, B.J.Pavelich and K.McGarty, *Can.J.Chem.*, **66**, 1589(1988)

6 A.Tomba Singh, *Ph.D Thesis*,**(2002**)

7 (a) G.Simonneaux, V.Schunemann, C.Morice, L.Carel, L.Toupet, H.Winker, A.X.Trautwein, and F.A.Walker, *J.Am.Chem.Soc.*, **122,** 43666(2000)

(b) M.K.Safo, M.J.N.Nesset, F.A.Walker, P.G.Debrunner, and W.R.Scheidt, *J.Am.Chem.Soc.*, **119**,9438(1997)

(c) F.A.Walker,.H.Nasri, I.Turowskatyrk, K.Mohanrao, C.T.Watson, N.V.Shokhirew P.G.Debrunner and W.R.Scheidt ., *J.Am.Chem.Soc.***118**,12109(1996)

(d) M.R.Safo, and F.A.Walker., *J.Am.Chem.Soc.*, **118,**7373(1996)

(e) M.K.Safo, F.A.Walker, A.M.Raitsimring, W.P.Walters, D.P.Dolata, P.G.Debrunner, and W.R.Scheidt., *J.Am.Chem.Soc.*, **116**, 7760(1992)

(f) M.K.Safo, G.P.Gupta, C.T.Watson, U.Simonis, F.S.Walker and W.R.Scheidt., *J.Am.Chem.Soc.*, **114**,7066(1992)

8 (a).A.Ghosh, I.Halvorsen, H.J.Nilsen, E.Steene, T.Wondimagegin, R.Lie, E.Vancaemelbacke, N.Guo, Z.Ou, and M.K.Kadish., *J.Phs.Chem.B.,* **105**,8120(2001)

(b) A.Ghosh, E.Gonzalez, and T.Vangberg., *J.Phys.Chem.B,* **103,** 1363(1999)

9 R.Harada, H.Okawa and T.Kojima., *Inorg.Chim.Acta.,* **358**, 489(2005)

Chapter-2

Experimental Section

2.1. Introduction

This chapter deals with the experimental techniques used and the synthesis of porphyrin and metalloporphyrins, purification of solvents and other reagents used in cyclic voltammetric and ESR studies.

2.2 Solvents

Common solvent and other reagents used at various stages of this work were purified according to the standard procedures described[1].

1) Chloroform: Drum samples were dried over $CaCl_2$ and distilled twice before being employed for synthesis, extraction and running column. For recrystallization and other physical measurements spectroscopic grade solvent was used.

2) Dichloromethane: Drum samples were refluxed over K_2CO_3 (anhydrous) for about 4 hours and distilled. This solvent has been used for synthesis, extraction and running column. For recrystallization and other physical measurements spectroscopic grade solvent was used

3) Methanol: Drum samples were refluxed over CaO(anhydrous) for about 6 hours and distilled with iodine and Mg turnings twice.

This solvent has been used for synthesis, extraction and running column. For recrystallization and other physical measurements spectroscopic grade solvent was used

4) Pyrrole: Pyrrole was purified by distillation under reduced pressure in the presence of KOH pellets and stored in a dark sealed bottle.

2.3. Oxidizing agent

Antimony pentachloride solution (1M solution in dichloromethane) was purchased from Aldrich Chemical Company and used directly.

2.4. Reagents and supporting electrolytes[2,3]

This section describes the methods of preparation of tetra-n-butylammonium perchlorate(TBAP)[1] and the complexes which were used during the course of our investigation. Some of the reagents were procured commercially.

i) Sodium perchlorate

Sodium perchlorate has been prepared[2] by neutralization of sodium carbonate (AnalR) with hydrogen perchloric acid(Qualigen, AR). After complete neutralization, the volume of the reaction mixture was concentrated and allowed to cool and sodium perchlorate crystallizes out. It was then recrystallized from distilled water, several times. The purity of the sample has been tested by running a cyclic voltammogram.

ii) Tetra-n-butylammonium perchlorate (TBAP)

A saturated solution of tetrabutylammonium iodide (Aldrich Chemical Company) has been prepared in distilled water. To this solution, sodium perchlorate was added, while tetrabutylammonium perchlorate precipitates out instantly. It has been stirred constantly till the formation of the precipitate and filtered fast. In order to avoid the liberation of iodine excess of sodium perchlorate was added. The precipitates have been suction filtered and dried by pressing between filter papers. After complete drying, tetrabutylammonium perchlorate was dissolved in methanol and reprecipitated out by adding distilled water. It was then filtered and dried as before, then recrystallized from methanol. Glassy crystals were formed. The purity of the sample has been tested by running a cyclic voltammogram.

2.5. Synthesis of Porphyrins

2.5.1.meso-5,10,15,20-Tetrakis(2,5-methoxyphenyl)porphyrin

meso-5,10,15,20-Tetrakis(2,5-dimethoxyphenyl)porphyrin[4] was prepared according to the method as described in the literature. In a 500 mL round bottom flask fitted with nitrogen bubbler 2,5-dimethoxy benzaldehyde(0.4952g, 2.98 mmol) and pyrrol (210 µl, 2.98 mmol) were dissolved in 300 mL of dichloromethane. After purging nitrogen for 10 min, the condensation of 2, 5-dimethoxy benzaldehyde and pyrrole was initiated by adding catalytic amount of $BF_3.OEt_2$ (120 µl, of 2.5M stock solution). The reaction mixture was stirred at room temperature for 1hour. The progress of the reaction was monitored by taking aliquots of the reaction mixture at regular intervals and oxidizing with p-chloranil and recording the absorption spectra which clearly confirmed the formation of porphyrin. After 1 hour p-chloranil (0.7327g, 2.98 mmol) was added and the reaction mixture was stirred in air for additional 1 hour. The solvent was removed under reduced pressure and the crude compound was purified by silica gel column chromatography using dichloromethane.

λ_{max} : 419 nm(S), 513nm, 546nm, 587nm, 642nm

2.5.2.meso-5,10,15,20-Tetrakis(o-nitrophenyl)porphyrin

meso-5,10,15,20-Tetrakis(o-nitrophenyl)porphyrin was prepared according to the method as described in the literature[4].

λ_{max} : 421 nm(S), 516nm, 551nm, 593nm, 649nm

2.5.3.meso-5,10,15,20-Tetrakis(p-hydroxyphenyl)porphyrin

meso-5,10,15,20-Tetrakis(p-hydroxyphenyl)porphyrin was prepared according to the method as described in the literature [5].

To a solution containing 18.3180g (150 mmol) of p-hydroxy benzaldehyde in 300 ml propionic acid 13.5 mL (106 mmol) of propionic anhydride were added. The resulting solution was allowed to reflux with stirring under the protection of bubbled nitrogen. Then 10.40 mL (150 mmol) of freshly distilled pyrrole in 10 mL of porpionic acid was added drop wise. After the addition the reaction mixture was stirred for further 30 min, and then 300 mL of 90% ethanol was added under vigorous stirring. The mixture was cooled to room temperature and kept at 15°C overnight. The tarry mixture was filtered and the solid product was washed repeatedly with a mixture of ethanol and propionic acid (1:1in volume), then with hot water until the rinsed solution were no longer dark. The filter cake was dried in air overnight, then at 150°C for 2 hour. The purple coloured crystalline meso-5, 10,15,20-Tetrakis(p-hydroxyphenyl)porphyrin were obtained. .

λ_{max} : 421 nm(S), 518nm, 555nm, 593nm, 649nm

2.5.4.meso-5,10,15,20-Tetrakis(pyridyl)porphyrin

meso-5,10,15,20-Tetrakis(pyridyl)porphyrin was purchased from Sigma-Aldrich chemical and was used directly.

2.6. Synthesis of metalloporphyrins

2.6.1. Vanadyl meso-5,10,15,20-Tetrakis (2,5-methoxyphenyl) porphyrin VO[T(2,5-$(OCH_3)_2$)PP][6]

The reaction was carried out with a mixture of 13.5 mL of glacial acetic acid, 6.5 mL of pyridine, 297mg(1.37mmol) of vanadyl sulphate and 358.21mg(0.42mmol) meso-5,10,15,20-Tetrakis(2,5-dimethoxyphenyl)porphyrin [T(2,5-$(OCH_3)_2$)PP] were taken in a 100 mL round bottom flask and was refluxed until the reaction was essentially complete (usually 4 to 5 hour). The crude product was cooled and washed with water thrice and the crude compound was purified by running through a silica gel column using dichloromethane.

Vanadyl meso-5,10,15,20-Tetrakis (o-nitrophenyl) porphyrin VO[T(*o*-NO_2)PP], Vanadyl meso-5,10,15,20-Tetrakis(p-hydroxyphenyl)porphyrin VO[T(*p*-OH)PP] and Vanadyl meso-5,10,15,20-Tetrakis(pyridyl)porphyrin VO[TpyP] were prepared according to the above method given in the literature[6].

VO[T(2,5-$(OCH_3)_2$)PP]

λ_{max} in dichloromethane : 425 nm. 546nm

VO[T(*o*-NO_2)PP]

λ_{max} in dichloromethane: 426 nm, 551 nm

VO[T(*p*-OH)PP]

λ_{max} in dichloromethane: 428 nm, 550 nm

VO[TpyP])

λ_{max} in dichloromethane: 420 nm, 545 nm.

2.6.2. Manganese meso-5,10,15,20-Tetrakis (2,5-methoxy-phenyl) porphyrin Mn[T(2,5-$(OCH_3)_2$)PP][6]

The reaction was carried out with a mixture of 335mg(1.37mmol) of manganese (II) acetate in methanol and 358.21mg(0.42mmol) of meso-5,10,15,20-Tetrakis (2,5-dimethoxyphenyl) porphyrin [T(2,5-$(OCH_3)_2$)PP] in chloroform The solution was taken in a 100 mL round bottom flask and refluxed until the reaction was essentially completed, usually around 5 hour. T he Crude product was cooled and washed with water thrice, the crude compound was purified by running a silica gel column chromatography using dichloromethane.

Manganese meso-5,10,15,20-Tetrakis (o-nitrophenyl) porphyrin Mn[T(*o*-NO_2)PP],, Manganese meso-5,10,15,20-Tetrakis (p-hydroxyphenyl) porphyrin Mn[T(*p*-OH)PP] and Manganese meso-5,10,15,20-Tetrakis(pyridyl)porphyrin Mn[TpyP]) were prepared according to the above method given in the literature[6].

Mn[T(2,5-$(OCH_3)_2$)PP]

λ_{max} in dichloromethane : 411 nm. 480nm (Soret), 575 nm, 607 nm

Mn[T(*o*-NO_2)PP]

λ_{max} in dichloromethane: 414 nm. 480nm (Soret), 584 nm, 620 nm

Mn[T(*p*-OH)PP]

λ_{max} in dichloromethane: 417 nm. 480nm (Soret), 585 nm, 623 nm

Mn[TpyP])

λ_{max} in dichloromethane: 417 nm. 475nm (Soret), 575 nm, 609 nm.

2.6.3. Cadmium and copper porphyrins[6]

Cadmium meso-5,10,15,20-Tetrakis (2,5-methoxyphenyl) porphyrin Cd[T(2,5-(OCH_3)$_2$)PP]

The reaction was carried out with a mixture of 335mg(1.37mmol) of cadmium (II) acetate in methanol and 358.21mg(0.42mmol) of meso-5,10,15,20-Tetrakis(2,5-dimethoxyphenyl)porphyrin [T(2,5-(OCH_3)$_2$)PP] in chloroform. The solution was taken in a 100 mL round bottom flask and refluxed until the reaction was essentially completed, usually around 5 hour. The Crude product was cooled and washed with water thrice, the crude compound was purified by running a silica gel column chromatography using dichloromethane.

Cadmium meso-5,10,15,20-Tetrakis (o-nitrophenyl) porphyrin Cd[T(*o*-NO_2)PP], Coper meso-5,10,15,20-Tetrakis (2,5-methoxyphenyl) porphyrin Cu[T(2,5-(OCH_3)$_2$)PP] and Copper meso-5,10,15,20-Tetrakis (o-nitrophenyl)porphyrin Cu[T(*o*-NO_2)PP] were prepared according to the above method given in the literature[6].

Cd[T(2,5-$(OCH_3)_2$)PP]

λ_{max} in dichloromethane : 427 nm. 549nm

Cd[T(*o*-NO_2)PP]

λ_{max} in dichloromethane: 429 nm, 555 nm

Cu[T(2,5-$(OCH_3)_2$)PP]

λ_{max} in dichloromethane : 422 nm. 542nm

Cu[T(*o*-NO_2)PP]

λ_{max} in dichloromethane: 424 nm, 556 nm

2.7. Instrumentation

2.7.1. Electron Paramagnetic Resonance (EPR)

EPR measurements were done using JEOL JES TE100 EPR spectrometer working at X band frequencies having 100 kHz field modulation at Pondicheery University, Pondicheery.. Oxidation was carried out in ESR tube by adding drops of 1M $SbCl_5$. All measurements were done after deaerating by bubbling nitrogen gas through the solution in the tube. The g values were determined by using solid DPPH as reference (g = 2.0036).

2.7.2. Cyclic voltammetric measurements

Redox potentials were determined using CHI 620B Electrochemical Analyzer, NEHU, Shillong, Meghalaya,India. The electrolytic cell is comprised of the following. A CHI(102) platinum electrode was used as a working electrode. An Ag/AgCl electrode was employed as a reference electrode. A platinum wire was used as an auxiliary electrode. Dry dichloromethane was used as the solvent. The amount of 0.1M of tetra-n-butylammonium perchlorate (TBAP) was used as supporting electrolyte. The solvent in the electrolyte cell was deaerated with oxygen free dry nitrogen gas before any measurement had been done and nitrogen blanket above the solution has been maintained. Calibration of $E_{1/2}$ values and diffusion current were made by using a known concentration of pure ZnTPP in dichloromethane/TBAP(0.1M) medium.

2.7.3. UV spectroscopy

Absorption spectroscopy was measured by BECKMAN 650DU Spectrophotometer, NEHU, Shillong, Meghalaya, India. Visible spectrums were measured in between the range 350-750 nm. Oxidations were carried out in quartz cuvette by adding drops of 1M $SbCl_5$

References

1. A.I.Vogel, *A text book of practical organic Chemistry*, fourth Edition [ELBS] Longman, London, 1978
2. *Hand book of Preparative Inorganic Chemistry*, Edited by G.Brauer (Academic press, New York, 1965), **Vol.II**. pp1185.
3. *Inorganic Synthesis*, Editor-in-Chief: Therald Moellur (McGraw Hill, 1975), **Vol.5**, pp154.
4. (a) I.Gupta, and M.Ravikanth., *Tetraheron*, **59**, 6131(2003),

   (b) I.Gupta, and M.Ravikanth., *Tetr.Lett*, **43**,9453(2002),

   (c) J.S.Lindsey, H.C.Hsu, and I.C.Schreimen., *Tetra.Lett.*, **27**,4969(1989),

   (d) R.W.Wagner, D.S.Lawrence, and J.S.Lindsey., *Tetra.Lett.*, **28**, 3069(1987).
5. Z.Jing, G.Yang, C.Shaokui, Z.Wennan, and W.Dongmai., www.chemistry.mag.org/cij/2002/048039.htm. **8**,39(2002).
6. J.S.Erdman, V.G.Ramsey, N.W.Ka;emda, ,and W.E.Hanson., *J.Am.Chem.Soc.*,**78**,5844(1956). b) A.D.Alder, F.R.Longo, F.Kampas, and J.Kim., *J.Inor.Nucl.Chem.*, **32**,2443(1970).

CHAPTER 3

CYCLIC VOLTAMMETRIC STUDIES OF SOME VANADYL PORPHYRINS

3.1. INTRODUCTION

Cyclic voltammetry has been used extensively in unlocking the redox processes in porphyrin and metalloporphyrin systems. The structure of the free base porphyrin and metalloporphyrins are presented in figure.3.1.1a and fig.3.1.1.b. The success of the cyclic voltammetric study in porphyrins and metalloporphyrins is reflected in the volume of research papers published in the literature[1-8]. We present here a brief introduction of the electrochemical behavior of some metalloporphyrins (in general). One can tune to the variation in the redox potentials of metalloporphyrins depending on the peripheral substituents and the central metal atom.

Generally, a metalloporphyrin may posses D_{4h} or C_4 symmetry (ordinarily). The HOMO (Highest occupied molecular orbital) a_{1u}, a_{2u} is nearly degenerate while the LUMO (Lowest unoccupied molecular orbital) e_g is truly degenerate. On oxidation, electrons are removed from the HOMO levels. The redox process may

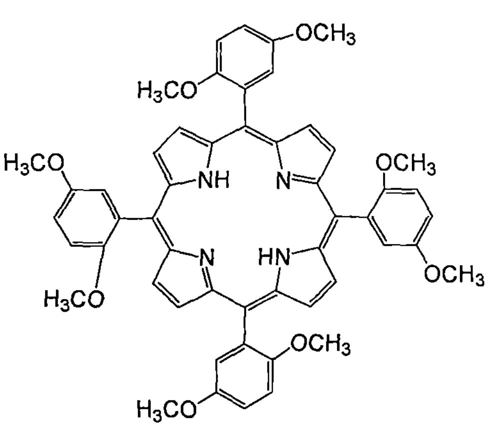

meso-5,10,15,20-Tetrakis(2,5-dimethoxyphenyl)porphyrin
[T(2,5-(OCH$_3$)$_2$)PP]

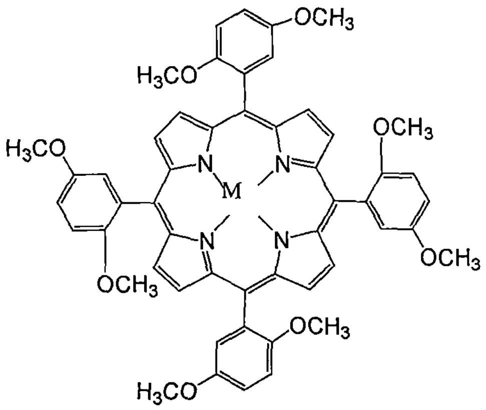

$M = VO^{2+} \longrightarrow VO[T(2,5\text{-}(OCH_3)_2)PP]$
$M = Mn^{2+} \longrightarrow Mn[T(2,5\text{-}(OCH_3)_2)PP]$
$M = Cd^{2+} \longrightarrow Cd[T(2,5\text{-}(OCH_3)_2)PP]$

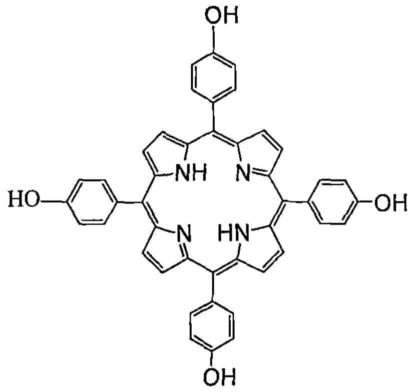

meso-5,10,15,20-Tetrakis(*p*-hydroxyphenyl)porphyrin
[T(*p*-OH)PP]

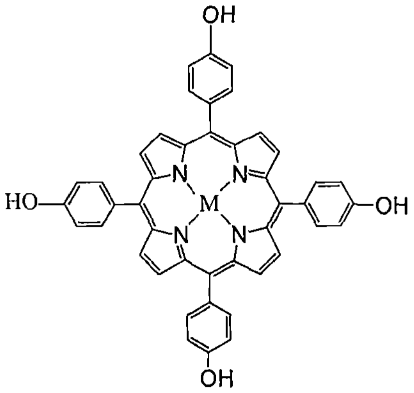

$M = VO^{2+} \longrightarrow VO[T(p\text{-}OH)PP]$
$M = Mn^{2+} \longrightarrow Mn[T(p\text{-}OH)PP]$

3.1.1a. Structure of free base porphyrin and metalloporphyrin

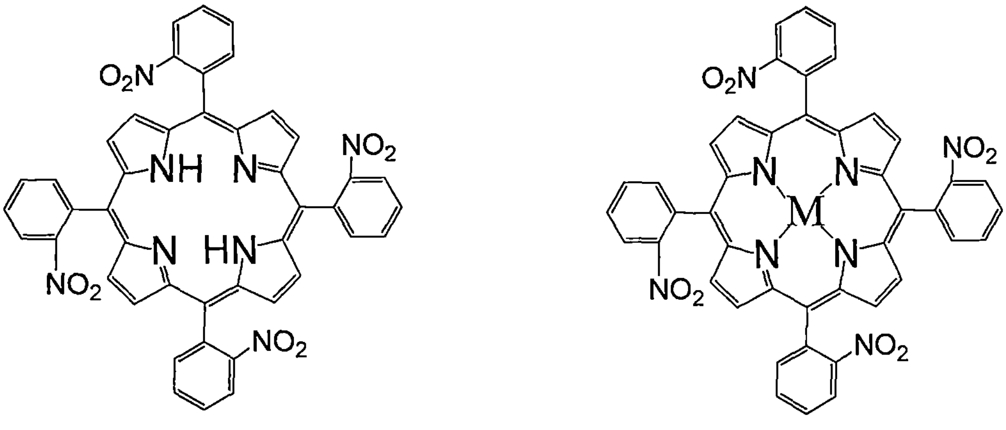

meso-5,10,15,20-Tetrakis(*o*-nitrophenyl)porphyrin
[T(*o*-NO$_2$)PP],

$M = VO^{2+} \longrightarrow VO[T(o\text{-}NO_2)PP]$,
$M = Mn^{2+} \longrightarrow Mn[T(o\text{-}NO_2)PP]$,
$M = Cd^{2+} \longrightarrow Cd[T(o\text{-}NO_2)PP]$,

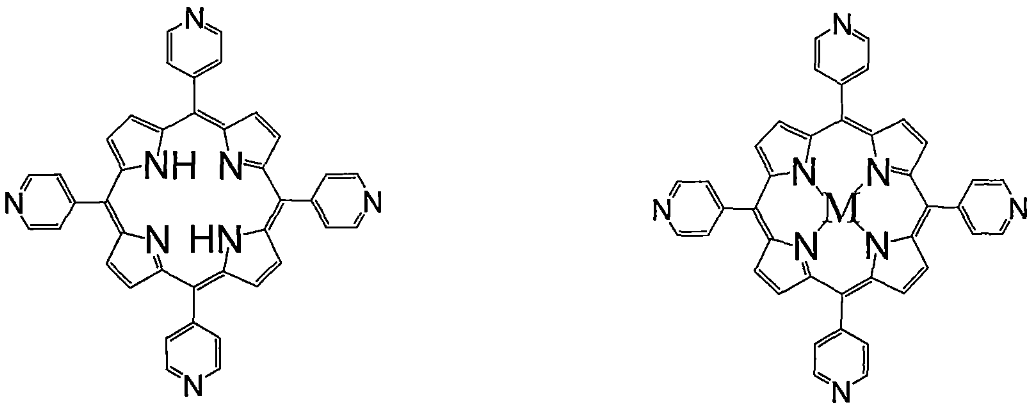

meso-5,10,15,20-Tetrakis(pyridyl)porphyrin
[TpyP]

$M = VO^{2+} \longrightarrow Vo[TpyP]$
$M = Mn^{2+} \longrightarrow Mn[TpyP]$

3.1.1b. Structure of free base porphyrin and metalloporphyrin

occur (i) in the porphyrin ligand or (ii) in the central metal atom or (iii) in both systems. The first process occurs when the central metal atom is electro inactive to the redox process, such a Zn, Cu etc., in the potential range used. The second and the third processes occur when the central metal atom is electro active to the redox process such as Fe, Co, Mn etc. One can understand by considering the occupied energy levels of π- electrons of the ligand and the d electrons of the metal atom (fig.3.1.2). In case (i) the HOMO energy level of the porphyrin ligand is higher than that of the metal. Hence the electron transfer will take place on the ligand. In case (ii) the HOMO of the metal atom is higher than that of the ligand. In case (iii) both ligand and metal atom energy levels are more or less same. Hence the electron transfer will take place in both systems. In this thesis we will focus mainly on the vanadyl porphyrins which falls under case(i) redox process of a metalloporphyrins containing a bivalent metal, one can represent as follows[1]:

Oxidation

$$M(II)P \xrightarrow[E^{ox}(I)]{-e} M(II)P^{+} \xrightarrow[E^{ox}(II)]{-e} M(II)P^{++}$$

Reduction

$$M(II)P \xrightarrow[E^{red}(I)]{+e} M(II)P^{-} \xrightarrow[E^{red}(II)]{+e} M(II)P^{--}$$

$$\Delta_{ox} = E^{ox}(II) - E^{ox}(I)$$

$$\Delta_{red} = E^{red}(II) - E^{red}(I)$$

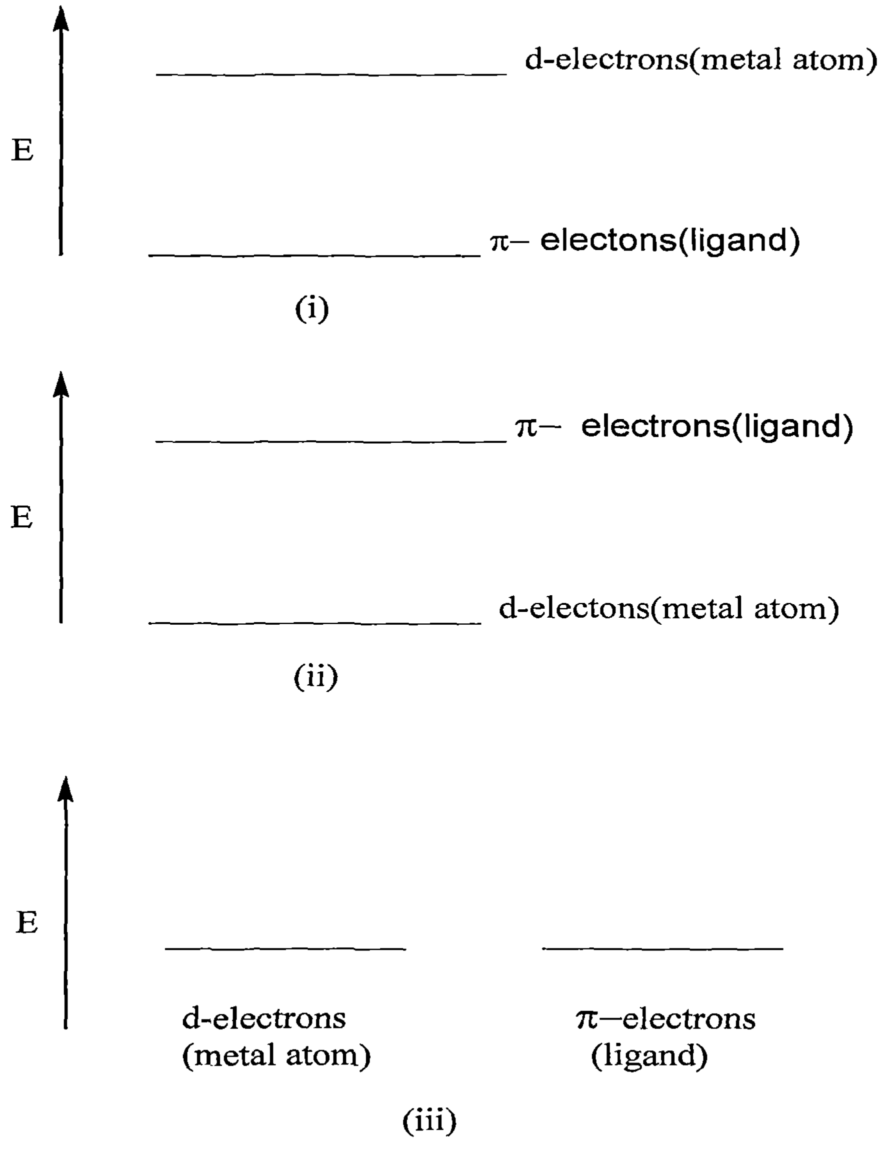

Fig.3.1.2.HOMO representation for metalloporphyrins

For redox processes in the ring, it has been observed that either Δ_{ox} or Δ_{red} are observed to be more or less constant.

$$\Delta_{ox} \approx 0.3eV$$

$$\Delta_{red} \approx 0.5eV$$

Also, the quantity,

$\delta = E_{ox} - E_{red}$ (1) has been observed to be more or less constant for a variety of metalloporphyrins (2.00 ±0.15V) although the absolute magnitude of the potentials vary widely. Independence of Δ_{ox} , Δ_{red} and δ of the metal is explained in terms of negligible mixing of the metal orbitals and the orbitals of the porphyrin ligand. The metal ion exerts an inductive columbic effect on the ligand π orbitals through σ frame work. This influence affects only the absolute values of π energy levels but not the relative values ie, the difference in the energies between HOMO and LUMO, using Parise-Parr-Pople π electron energies, the values Δ_{ox}, Δ_{red} and δ have been estimated which agree reasonably well with the corresponding experimental data but fails to correlate when redox processes occur in the metal center.

3.2. PRINCIPLE OF CYCLIC VOLTAMMETRY[9-12]

It is an electrochemical technique used as an analytical technique to determine the redox potentials. The electrolytic cell comprises of three electrodes (fig.3.2.1) the working electrode (a platinum disc electrode), an auxiliary electrode (a platinum wire) and a saturated calomel electrode or Ag/AgCl electrode as reference electrode. The working electrode is scanned with a triangular wave (fig.3.2.2.) potential. The triangular wave potential can be arbitrarily fixed between an initial and a final potential which are called switching potentials. Normally, a current-voltage cure known as voltammogram is obtained in an unstirred solution containing a supporting electrolyte and the sample.

For a single-step reversible electron transfer process a voltammogram containing two peaks one on the oxidation side (E^{ox}) and its corresponding reduction.

Peak (E^{red}) on the reverse side is obtained. These two peaks together are called a couple. One can represent a simple redox system by equation.

$$R \underset{+e}{\overset{-e}{\rightleftharpoons}} R^{+} \qquad \text{--------------------- (3.2.1)}$$

While sweeping the working electrode with a positive triangular wave, a peak is obtained at a potential E_a ($\approx E^{ox}$)

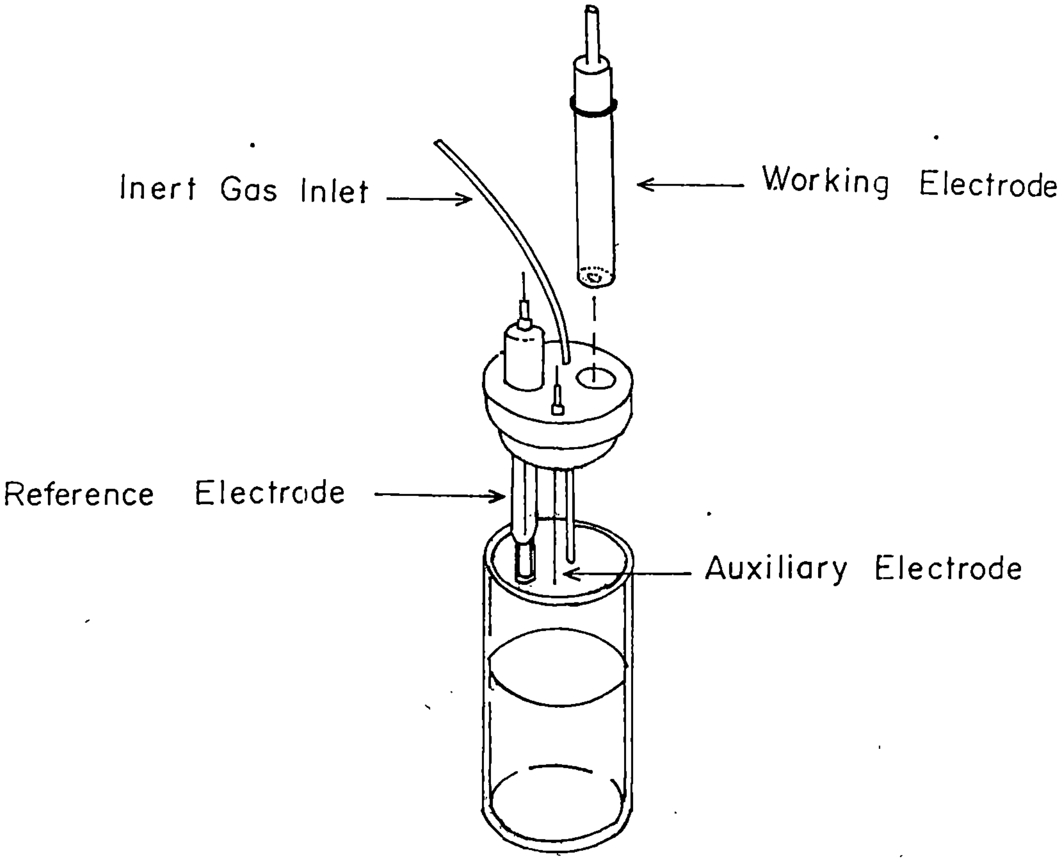

Fig.3.2.1. Electrochemical cell for quality cyclic voltammetry experiment

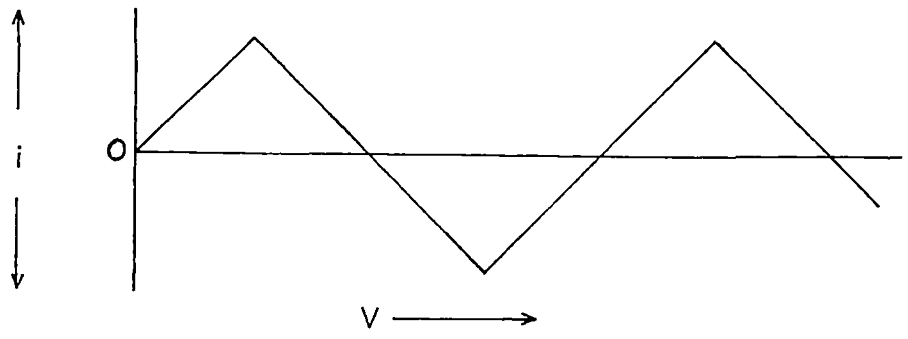

Fig.3.2.2. Triangular wave

Corresponding to the process $R \rightarrow R^{+\cdot}$. In the reverse sweep the species R^+ is reduced back to R giving rise to the corresponding reduction peak at a potential $E_c(\approx E^{red})$. The half-wave potential is given by the expression

$(E_a+E_c)/2 = E_{1/2}$------------------- (3.2.2)

Expressing in terms of polarographic half-wave potential

$Ep = E_{1/2} - 1.11(RT/nF)$

$= E_{1/2} - 1(0.0285/nF)$-------------------------(3.2.3)

where n = number of electron involved in the electrode reaction

T = 298 K

Peak to peak difference

$\Delta E = E_a - E_c = (0.059/n)V$-------------------------(3.2.4)

at 25°C

The peak current for a reversible process is given by Randles-Sevick equation

$I_p = 2.69 \times 10^5 n^{3/2} A C D^{1/2} \gamma^{1/2}$ ----------------------------(3.2.5)

Where γ is the scan rate in volts per second.

Thus, for a reversible process

$I_c/I_a = 1$ ---(3.2.6)

Where I_c = Cathodic peak current

I_a = anodic peak current

3.3. EXPERIMENTAL DETAILS

The synthesis of meso porphyrin [T(2,5–$(OCH_3)_2$)PP], [T(o-NO_2)PP], [T(p-OH)PP], TPyP and its vanadyl complexes are discussed in detail in chapter II. Dichloromethane and tetra-n-butylammonium perchlorate were used as solvent and supporting electrolyte respectively. Cyclic voltammetric studies were done on vanadyl porphyrins [VO[T(2,5–$(OCH_3)_2$)PP], VO[T(*o*-NO_2)PP], VO[T(*p*-OH)PP], and VO[TpyP]. All the CV measurements were done with 10^{-3} M solutions of the metalloporphyrins.

Note: Nitrogen gas is bubbled through the electrolytic solution before recording to expel the dissolved oxygen. Nitrogen blanket is maintained above the solution while recording the voltammogram.

3.4.RESULS AND DISCUSSION

3.4.A.RESULTS

All CV results are summarized in the table (3.1)

VO[T(2,5–$(OCH_3)_2$)PP] The voltammogram shows two redox couples(fig.3.4.1) with their $E_{1/2}$ values 1.042V and 1.225V respectively. The first oxidation occurs at 1.085V and its corresponding reduction occurs at 0.999V. Its ΔE value is 0.086V. The second oxidation occurs at 1.2744V and its corresponding reduction occurs at 1.1749V. Its ΔE value is 0.0995V. The current ratio $I_a/I_c \approx 1$

VO[T(*p*-OH)PP], The voltammogram(fig.3.4.2) exhibits the first oxidation at 0.6372V with its corresponding reduction at 0.4745V. Its ΔE value is 0.1627V, $E_{1/2}$ = 0.5559V and $I_a/I_c \approx 1$. The second oxidation occurs at 1.2852V while its corresponding reduction occurs at 0.9482V. The $E_{1/2}$ value is 1.1167V, ΔE = 0.337V and its $I_a/I_c > 1$.

VO[T(*o*-NO$_2$)PP], The voltammogram exhibits some additional peaks(fig.3.4.3) otherwise contain regular redox couples which are expected. The first oxidation occurs at 0.730V with its corresponding reduction at 0.553V. The ΔE = 0.177V, $E_{1/2}$ = 0.6415V and its $I_a/I_c \approx 1$. The second oxidation occurs at 1.2271V with its corresponding reduction peak at 1.055V. Its ΔE = 0.1721V, $E_{1/2}$ = 1.1411V and $I_a/I_c \approx 1$.

VO[TPyP] : The voltammogram comprises of two redox couples. The first oxidation occurs at 0.6896V with its corresponding reduction at 0.5185V. The second oxidation peak occurs at 1.0484V with its corresponding reduction peak at 0.8976V (fig.3.4.4)

3.4. B. DISCUSSION

The voltammogram of [VO[T(2,5–(OCH$_3$)$_2$)PP] indicates that the oxidation potentials are slightly higher than that of the VOTPP by about 0.085V and 0.054V respectively. But the oxidation potentials are slightly lower than that of the [VO[T(*m*–OCH$_3$)PP] by about 0.075V and 0.076V and to that of the [VO[T(*p*–OCH$_3$)PP] by about 0.075V and 0.076V. The reason for lowering the oxidation potentials in the case of [VO[T(2,5–(OCH$_3$)$_2$)PP] may be because of symmetrical substitution of the phenyl ring which puts it more or less in the similar geometry to that of VOTPP. Although the shifts in the potential either way are small and they are quite uniform. This gives us some thoughts to suggest that there are some changes in the geometry of the molecule on substitution which affect the energy levels (HOMO) of the molecule hence shifts in the redox potentials occurs. However, to supplement this point it requires rigorous theoretical and experimental works which is not possible for us to do at the moment. Perhaps, this is due to the interaction of metal d-orbital and the porphyrin ligand orbital in ruffle and saddle distortion as suggested by Walker et al[13] and Gosh et al[14] In fact the voltammogram is of successive one electron transfer of the porphyrin ligand and are reversible. The redox process is represented by the following scheme:

$$\begin{tikzcd}
\mathrm{VO[T(2,5\text{-}(OCH_3)_2PP]} \arrow[r, shift left, "\text{-e(1.085V vs SCE)}"] & \mathrm{(VO[T(2,5\text{-}(OCH_3)_2PP])^{+}} \arrow[l, shift left, "\text{+e(0.999V vs SCE)}"] \arrow[d, shift left, "\text{-e(1.274V vs SCE)}"] \\
 & \mathrm{(VO[T(2,5\text{-}(OCH_3)_2PP])^{2+}} \arrow[u, shift left, "\text{+e(1.1749V vs SCE)}"]
\end{tikzcd}$$

The voltammogram of the VO[T(*p*-OH)PP] is not a straight forward successive one electron transfer process. The first oxidation potential and its corresponding reduction potential are lower than that of VOTPP, while the second oxidation shows very strong oxidation peak current. The peak current corresponds to more than one electron transfer. Similar trends were observed in the case of ZnTDP by earlier workers. Clearly, the second oxidation involved a process which is irreversible along with the reversible process. Evans et al[15] indicated it as due to formation of secondary oxidation states involving the phenolic groups. Murray and co-workers[16] attributed it as due to oxidative electro polymerizations. On subsequent scanning the peak current decreases leading to film formation at the electrode (fig.3.4.2). The electron donating group (-OH) increases the electron density of the macrocycle. This makes the removal of electron easier. Thus, the oxidation potential decreases.

The redox process of VO[T(*o*-NO_2)PP] is in line with the redox process of the VO[T(2,5–$(OCH_3)_2$)PP]. The first oxidation occurred at a lower potential than that of the VOTPP. This is quite surprising because we expected it to occur at a higher potential. The electron withdrawing -NO_2 should make the ring π-electron density lower making oxidation more difficult. This is what we observed in our earlier work[17] in VO[T(m-NO_2)PP]. One possible reason could be, the -NO_2 in meta position which is in more sterically hundred position making it more strain to take part in the porphyrin ring resonance. Thereby, no effective electron withdrawal from the ring takes place. The result is no shift in potential to a higher value. This requires more experimental investigations to prove the point. However, the system undergoes two successive oxidation processes involving one electron transfer in each step which is represented as follows:

$$\begin{tikzcd}
VO[T(o\text{-}NO_2)PP] \arrow[r, shift left, "-e(0.730V\ vs\ SCE)"] & (VO[T(o\text{-}NO_2)PP])^{+} \arrow[l, shift left, "+e(0.553V\ vs\ SCE)"] \arrow[d, shift left, "-e(1.227V\ vs\ SCE)"] \\
 & (VO[T(o\text{-}NO_2)PP])^{2+} \arrow[u, shift left, "+e(1.055V\ vs\ SCE)"]
\end{tikzcd}$$

VO[TPyP] undergoes oxidation in steps similar to that of the VOTPP oxidation. The oxidation potentials are lower than that of the VOTPP. The substituents enrich the π-electron density making oxidation more easier. The oxidation process is represented as

$$\begin{tikzcd}
VO[TpyP] \arrow[r, shift left, "-e(0.6896V\ vs\ SCE)"] & (VO[TpyP])^{+} \arrow[l, shift left, "+e(0.518V\ vs\ SCE)"] \arrow[d, shift left, "-e(1.0484V\ vs\ SCE)"] \\
 & (VO[TpyP])^{2+} \arrow[u, shift left, "+e(0.8976V\ vs\ SCE)"]
\end{tikzcd}$$

3.5. CONCLUSION

From the results of the cyclic voltammetric investigation of VO[T(2,5–$(OCH_3)_2$)PP], VO[T(o-NO_2)PP], VO[T(p-OH)PP], and VO[TPyP] we put forward the following observations:

When the metal centre is non electro-active such as vanadyl the redox process takes place in the porphyrin ligand system.

When substitutions in the phenyl ring of the porphyrin ligand are symmetrical with electron donating group, the oxidation potentials are further lowered. The reverse is also true.

It seems the substitution in the ortho-position of the phenyl ring of the porphyrin ligand is more sterically hindered and strain that the substituents do not contribute much to the resonance. Thus, the oxidation potentials of VO[T(o-NO_2)PP] is slightly less than that of VOTPP (may be due to more puckered structure).

In general it appears that substitution on the phenyl ring causes distortions which affect the redox potentials.

It is most likely that lowering in oxidation potentials could be due to interactions of metal d_{xy} orbital with porphyrin (a_{2u}) orbital in ruffle distortion and metal dx^2-y^2 orbital with porphyrin (a_{2u}) in saddle distortion.

In some cases such as VO[T(p-OH)PP] secondary electrode reaction takes place resulting in the film formation on surface of the electrode.

Table: **3.1. Cyclic voltammetric data for vanadyl porphyrins at room temperature**

Solvent : Dichloromethane
Supporting electrolyte : TBAP
Concentration : 10^{-3}M
Reference electrode : Ag/AgCl

System	Scan Rate (V/s)	Epa(1) V	Epa(2) V	Epc(1) V	Epc(2) V	ΔE(1) (Epa–Epc) V	ΔE(2) (Epa–Epc) V	$E_{1/2}(1)$ [(Epa+Epc)/2] V	$E_{1/2}(2)$ [(Epa+Epc)/2] V
VO[T(2,5–(OCH_3)$_2$)PP]	0.06	1.085	1.2744	0.999	1.1749	0.086	0.0995	1.0420	1.2246
VO[T(p-OH)PP]	0.05	0.6372	1.2852	0.4745	0.9482	0.163	0.3370	0.5559	1.1167
VO[T(o-NO_2)PP	0.1	0.730	1.2271	0.553	1.055	0.177	0.1721	0.6415	1.1411
VO[TPyPP]	0.01	0.6896	1.0484	0.5185	0.8976	0.171	0.1508	0.6040	0.9730

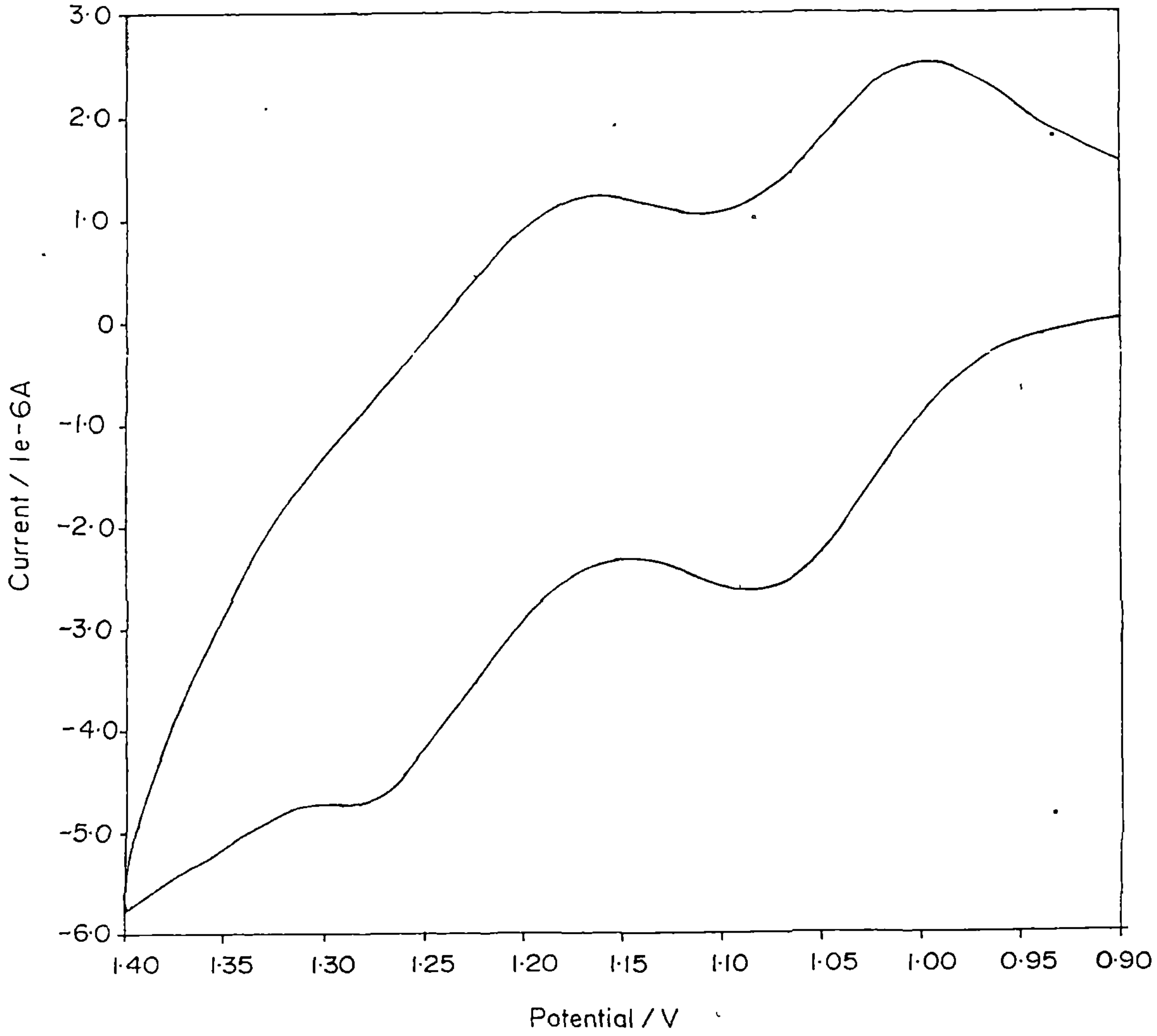

Fig. 3.4.1. Cyclic voltammogram of VO[T(2,5-$(OCH_3)_2$)PP] in CH_2Cl_2 containing 0.1M TBAP at room temperature. Scan rate 0.06 V/s.

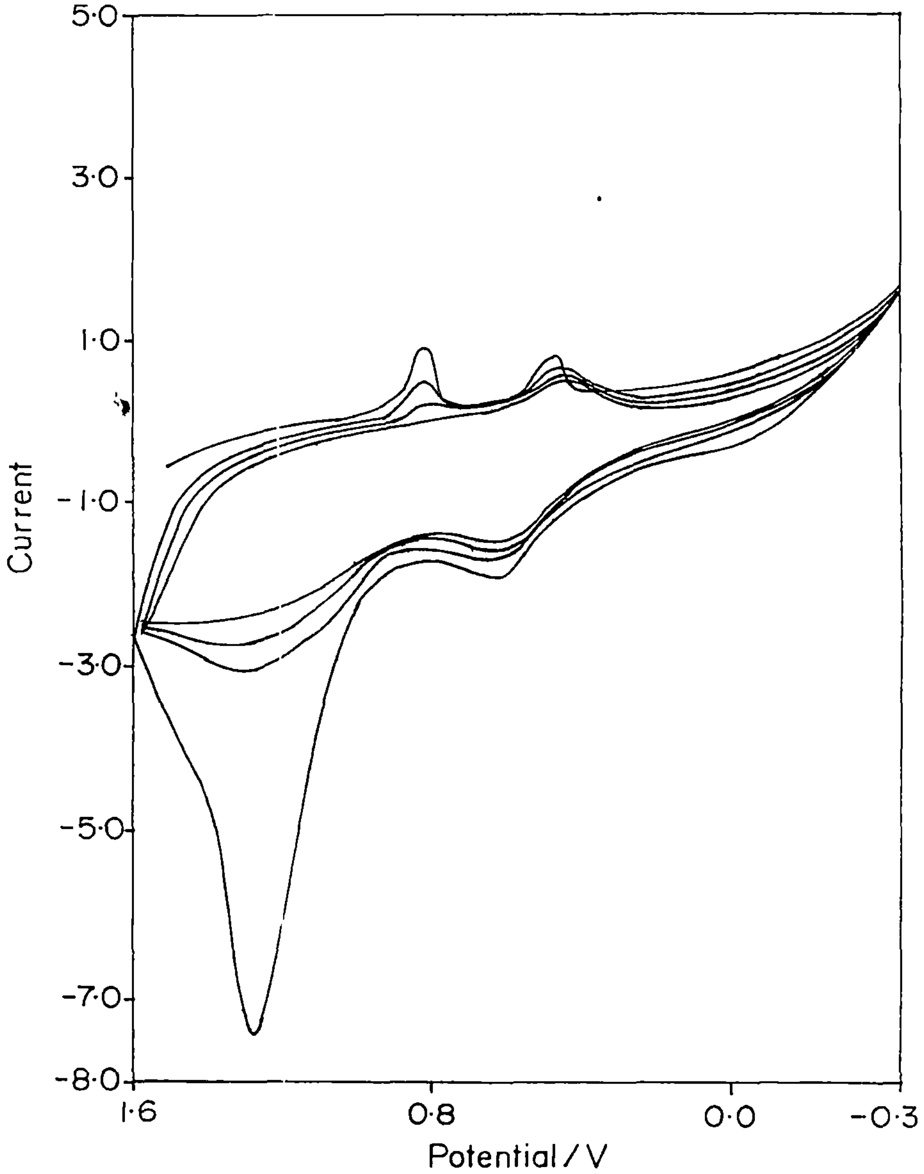

Fig. 3.4.2. Cyclic voltammogram of VO[T(*p*-OH)PP] in CH_2Cl_2 containing 0.1M TBAP at room temperature. Scan rate 0.05 V/s.

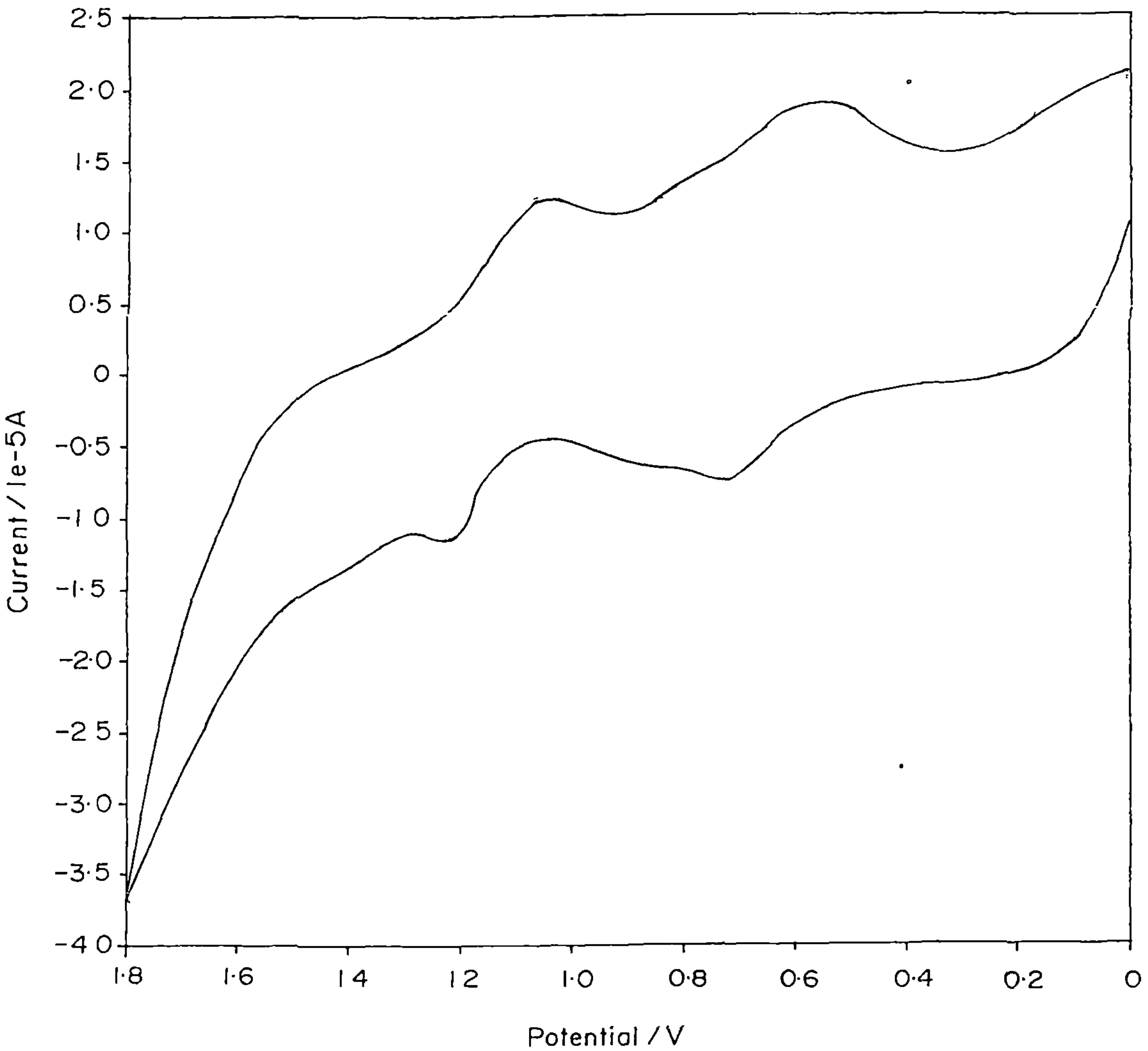

Fig. 3.4.3. Cyclic voltammogram of VO[T(o-NO_2)PP] in CH_2Cl_2 containing 0.1M TBAP at room temperature. Scan rate 0.1 V/s.

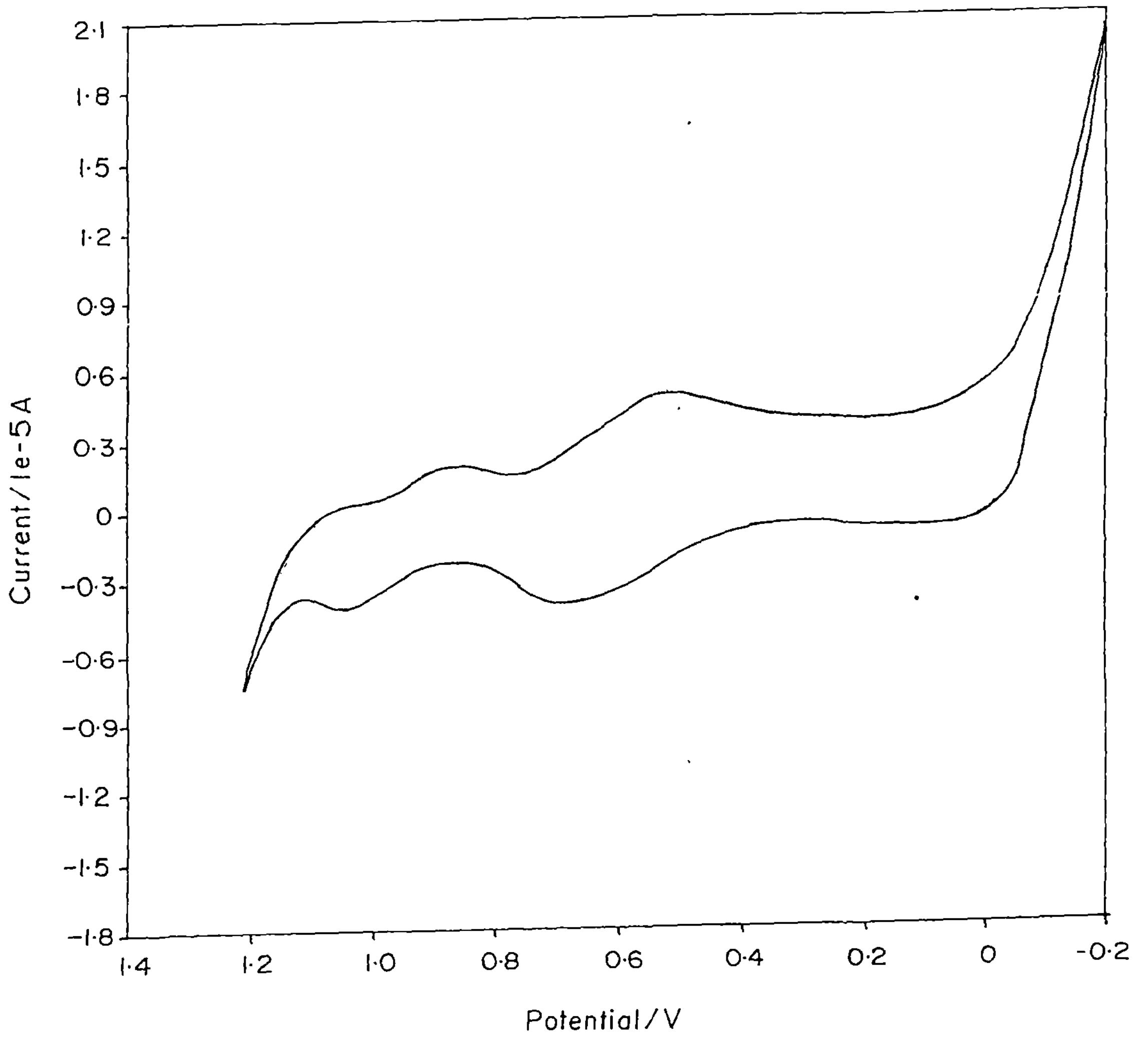

Fig. 3.4.4. Cyclic voltammogram of VO[TpyPP] in CH_2Cl_2 containing 0.1M TBAP at room temperature. Scan rate 0.01 V/s.

REFERENCES

1. R. H. Felton, in '*The Porphyrins*" edited by Dolphin(Academic press" , New York, 1979) **Vol.V**, p53
2. D. G. Davies, In *The Porphyrins*" edited by Dolphin(Academic press" , New York, 1979) **Vol.V**, p127
3. C. M. Newton and D. G. Devies, *J. Magn. Resonance*., **20(4),** 446(1975)
4. K. M. Kadish and M. Morrison, *Inorg. Chem.*,**15**, 930 (1976)
5. A. Girandean, H. J Callof and M. Gross, *Inorg. Chem.*, **18,** 201 (1979)
6. L. A. Bottomely, L. Olson, K. M. kadish, in *"Electrochemical and spectrochemical studies of Biological redox component"* Edited by K. M. Kadish (ACS advances, Washingston,1982), p279
7. R. Harada, H. Okawa and T. Kojima, *Inorg.Chim.Acta.*, **538,** 489 (2005)
8. I. Mayer, H. E. Toma, and K. Araki, *J. Elect.Ana. Chem.*, **590**,111(2006)
9. G. A. Mabboti, *J. Chem. Edn*, **60**, 697 (1983)
10. P. T. Kissinga and W. R.Heineman, *J. Chem. Edn.,* **60**, 702 (1983)

11. G. Canquis, V. D. Parker,in *"Organic Electrochemistry"* Edited by M. M. Baizer(Mancel Dekker, New York, 1973) p93

12. *Operations Mannual,* Bioanalytical System INC., West Lafayette, In,1983

13. G. Simonneaux, V. Schunemann, C. Morice, L. Carel, L. Toupet, H. Winkler, A. X. Trautwein, F. A. Walker., *J. Am .Chem. Soc.*, **122**, 4366 (2000)

14. A. Ghosh, I. Halvorsen, H. J. Nilsen, E. Steene, T. Wondimagegn, R. Lie, E. VanCaemelbecke, N. Guo, Z. Ou and K. M. Kaddish, *J. Phys. Chem.B,* **105,** 8120(2001)

15. T. A. Evans, G. S. Srivatsa, D. T. Sawyer and T. G. Traylor, *Inorg. Chem.*, **24**,4733 (1985)

16. A. Bettelhein, B. A. White, S. A. Raybuck and R. W. Muuray., *Inorg. Chem.*, **26**, 1009 (1987)

17. A. Tomba Singh and A. Lemtur., *Spect. Chim. Acta., Part A.,* **59**, 1549 (2003)

CHAPTER 4

CYCLIC VOLTAMMETRIC STUDIES OF SOME MANGANESE, CADMIUM AND COPPER PORPHYRINS

4.1. INTRODUCTION

In Manganese porphyrins the central metal atoms as well as the ligand are electro active. Therefore, redox processes may occur in both the ligand as well as in the metal. Therefore, such systems give some interesting situation to study. Further, many workers have reported the catalytic activities of manganese porphyrins in alkane oxidations.

On the other hand cadmium and copper porphyrins do not have electro active metal center. Therefore, oxidation occurs in the ligand system. However, these oxidations depend on the central metal atom as well as the substitution in the ligand system. Further, redox processes will reflect the type of bonding that exists between the metal and the ligand[1-9].

4.2. RESULTS OF MANGANESE PORPHYRINS

Voltammograms of manganese porphyrins that are recorded are presented (fig.4.2.1, 4.2.2, 4.2.3 and 4.2.4). The results are summarized in the table 4.1. In all four manganese porphyrins three redox couples are observed.

Mn[T(2,5-$(OCH_3)_2$)PP] gives oxidation potentials 0.798V, 0.964V and 1.460V with their corresponding reduction potentials 0.5997V, 0.727V and 1.289V. Their ΔE values are 0.198V, 0.217V and 0.171V. Also $E_{1/2}$ values are 0.6989V, 0.8455V and 1.3745V.

Mn[T(*p*-OH)PP]: The oxidation potentials are 0.7255V, 1.1872V, and1.2891V and their corresponding reduction potentials are 0.5675V, 0.8841V, and 1.1381.V, . ΔE values are 0.158V, 0.303V and 0.151V. Also $E_{1/2}$ Values are 0.6465V, 1.0357V, and 1.2136V

Mn[T(*o*-NO_2)PP] : The oxidation potentials are 0.6493V, 0.9240V and 1.1988V and their corresponding reduction potentials are 0.5789V, 0.8404V, and 1.1188V. ΔE values are 0.0704V, 0.0836V and 0.08V. $E_{1/2}$ values are 0.6141V, 0.8822V and 1.1588V.

Mn[TpyP] : Oxidation potentials are 0.8521V, 1.2024V and 1.4902V with their corresponding reduction potentials 0.6408V and 1.5402V. ΔE values are 0.2113V and 0.050V and $E_{1/2}$ values are 0.7465 and 1.5152V.

4.3. DISCUSSION OF CYCLIC VOLTAMMETRY OF MANGANESE PORPHYRINS

The oxidation potential 0.798V of Mn[T(2,5-$(OCH_3)_2$)PP] is attributed to the oxidation of Mn(II)→Mn(III), while 0.964V and 1.460V are the first and the second ligand oxidations respectively. Irrespective of the large ΔE values, they exhibit reversibility (Fig.4.3.1, 4.3.2, 4.3.3 and 4.3.4)

For Mn[T(*p*-OH)PP], the oxidation potential 0.7255 V is attributed to Mn(II)→Mn(III) oxidation while1.1872V and 1.2891V are the first and second ligand oxidations and are reversible. Another oxidation is observed at the potential 1.2891Vwithout its counterpart reduction peak. This oxidation seems to be occurring at the ligand but not reversible. This could be due to polymerization at the electrode surface[12]. It is also possible that due to polymerization oxidations potentials are observed to be at lower potentials compared to that of Mn[T(2,5-$(OCH_3)_2$)PP].

In Mn[T(*o*-NO_2)PP] the metal oxidation (Mn(II)→Mn(III)) occurs at 0.6493V while the ligand oxidations occur at 0.9240V and 1.1988V. We expected the oxidation potentials are to be shifted higher because $-NO_2$ is electron withdrawing group. Instead the potentials are shifted lower compared to Mn[T(2,5-

$(OCH_3)_2$)PP]. On a possible reason could be due to ruffling in the porphyrin ligand structure[10-13].

In the voltammogram of Mn[TpyP], three oxidations are observed with only two reduction peaks. The metal oxidation is observed at 0.8521V. Their E1/2 values are 0.050V and 0.746V. Only one redox couple for the ligand is observed. The oxidation potentials, are higher than that of Mn[T(*o*-NO_2)PP]. To understand these changes we need to investigate structural changes (porphyrin ligand ruffling) which are beyond the scope of this thesis.

4.4. CONCLUSIONS ON THE CYCLIC VOLTAMMETRY STUDIES OF MANGANESE PORPHYRINS

From the CV studies of the above mentioned Manganese, porphyrins we confirm the following observations;

i) In all four manganese porphyrins, Mn(II)→Mn(III) oxidation occurs although at slightly different potentials depending on the ligand.

ii) Variation in the oxidation potential is attributed mainly to the nature of substitutions in the phenyl ring and the ruffling of the ligand structure.

iii) In the case of Mn[T(*p*-OH)PP] polymerization at the surface of the electrode is observed.

4.5. RESULTS OF CYCLIC VOLTAMMETRY STUDIES OF CADMIUM AND COPPER PORPHYRINS

Cd[T(2,5-$(OCH_3)_2$)PP] give two redox couples at $E_{1/2}$ values 1.0486V and 1.2216V. Oxidation potentials are 1.0852V and 1.279V with their corresponding reduction potentials at 1.0120V and 1.1642 respectively. The ΔE values are 0.0732V and 0.1149V (fig, 4.5.1 and Table.4.2)

The voltammogram of Cd[T(*o*-NO_2)PP] show two oxidations at 0.7149V and 1.5324V with their corresponding reductions at 0.6027V and 0.9972V respectively. ΔE values are 0.1122V and 0.5352V and $E_{1/2}$ values are 0.6588V and 1.2648V respectively (fig,4.5.2 and Table.4.2).

Cu[T(2,5-$(OCH_3)_2$)PP] voltammogram give two oxidations at 0.638V and 0.910V with their corresponding reductions at 0.5346V and 0.8098V respectively. The ΔE values are 0.1034V and 0.1002V and $E_{1/2}$ values are 0.863V and 0.8599V (fig,4.5.3 and Table.4.2).

Cu[T(*o*-NO_2)PP] produces voltammogram consists of two oxidations at 0.7702V and 1.2145V with their corresponding reduction at 0.6607V and 1.0332V respectively. The ΔE values are 0.1095V and 0.1813V and $E_{1/2}$ values are 0.7154V and 1.1238 (fig, 4.5.4 and Table.4.2)

4.6 DISCUSSION OF CYCLIC VOLTAMMETRY OF CADMIUM AND COPPER PORPHYRINS

For cadmium porphyrins two ligand oxidations are observed with their potentials higher than that of Cd(II)TPP. On the contrary Cd[T(*o*-NO_2)PP] exhibits lower oxidation potentials. This is quite surprising and we do not know why? Perhaps due to distortion in the ligand structure.

In the voltammogram of Cu[T(2,5-$(OCH_3)_2$)PP], the oxidation potentials are lower than that of Cu(II)TPP. This is as expected and is due to the electron donating group (-OCH_3). On the other hand the first oxidation potential of Cu[T(*o*-NO_2)PP] is lower than that of Cu(II)TPP while the second oxidation potential is slightly higher (Table.4.2). This is due to the electron withdrawing group (-NO_2) and the structural conformation of the porphyrin ligand[10-13].

4.7. CONCLUSIONS ON THE CYCLIC VOLTAMMETRY STUDIES OF CADMIUM AND COPPER PORPHYRINS

From the electrochemical studies of cadmium and copper porphyrins we observe the following;

i) No redox processes occur at the metal center. The redox processes occur at the ligand.

ii) Cu[T(2,5-$(OCH_3)_2$)PP] shows lowering in the oxidation potentials due to electron donating group(-OCH_3). On the other hand Cu[T(*o*-NO_2)PP] show increase in the oxidation potentials due to the electron with drawing group(-NO_2).

iii) Variations in the oxidation potentials may also be dependent on the ligand structural ruffling.

Table:4.1 Cyclic voltammetric data for manganese porphyrins at room temperature

Solvent : Dichloromethane
Supporting electrolyte : TBAP
Concentration : 10^{-3}M
Reference electrode : Ag/AgCl

System/	Scan Rate (V/s)	Epa(1) V	Epa(2) V	Epa (3) V	Epc(1) V	Epc(2) V	Epc (3) V	ΔE(1) V	ΔE(2) V	ΔE (3) V	$E_{1/2}$(1) V	$E_{1/2}$(2) V	$E_{1/2}$ (3) V
Mn[T(2,5–$(OCH_3)_2$)PP]	0.1	0.798	0.964	1.460	0.5997	0.727	1.289	0.1983	0.217	0.1710	0.6989	0.8455	1.3745
Mn[T(p-OH)PP]	0.03	0.7255	1.1872	1.2891	0.5675	0.8841	1.1381	0.1580	0.3031	0.1510	0.6465	1.0357	1.2136
Mn[T(o-NO_2)PP	0.04	0.6493	0.9240	1.1988	0.5789	0.8404	1.1188	0.0704	0.0836	0.080	0.6141	0.8822	1.1588
Mn[TPyPP]	0.01	0.8521	1.2024	1.4902	0.6408	----	1.5402	0.2113	-----	0.050	0.7465	----	1.5152

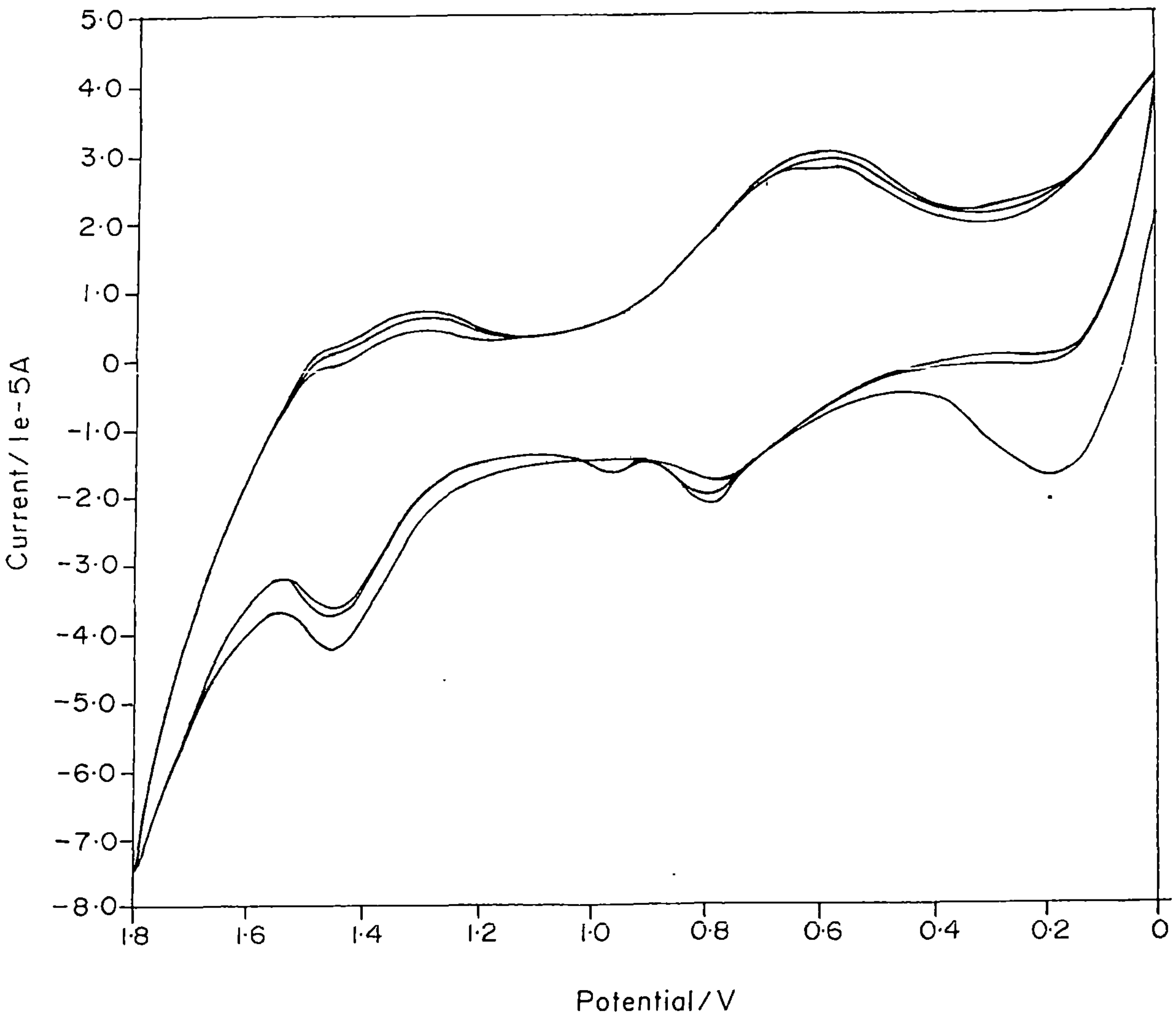

Fig.4.2.1. Cyclic voltammogram of Mn[T(2,5-$(OCH_3)_2$)PP] in CH_2Cl_2 containing 0.1M TBAP at room temperature. Scan rate 0.1V/s

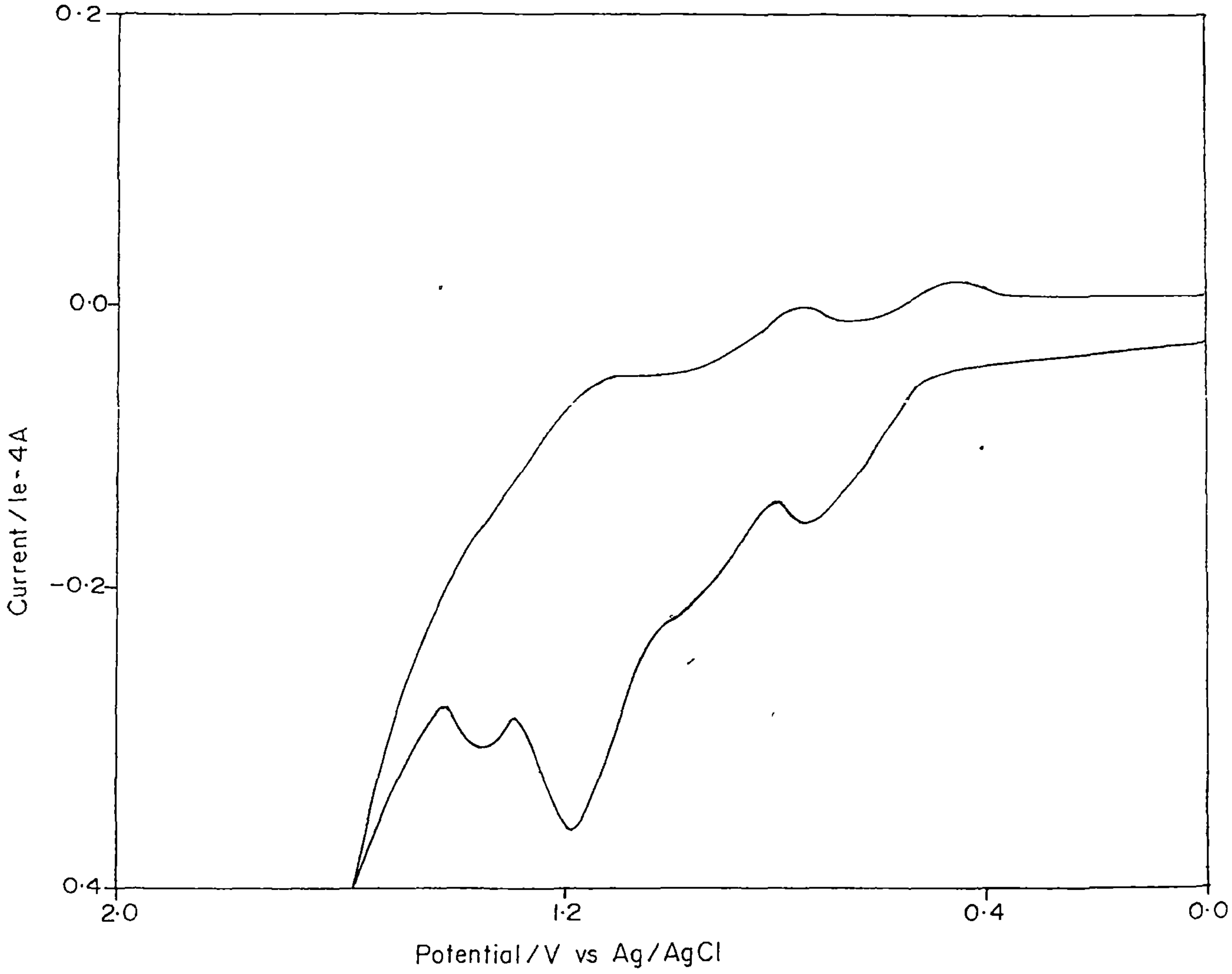

Fig.4.2.2. Cyclic voltammogram of Mn[T(*p*-OH)PP] in CH_2Cl_2 containing 0.1M TBAP at room temperature. Scan rate 0.03 V/s.

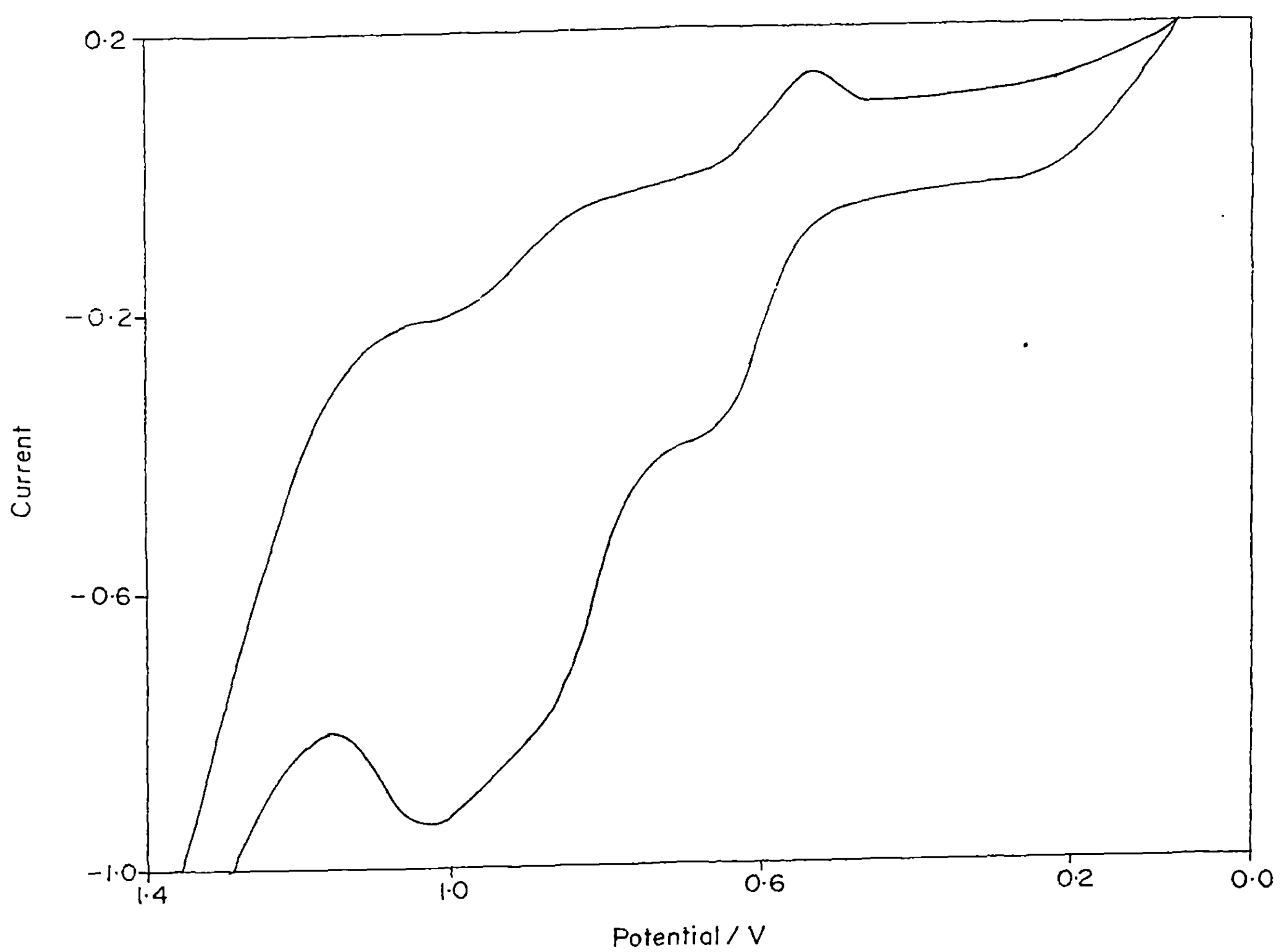

Fig.4.2.3. Cyclic voltammogram of Mn[T(*o*-NO_2)PP] in CH_2Cl_2 containing 0.1M TBAP at room temperature. Scan rate 0.04 V/s.

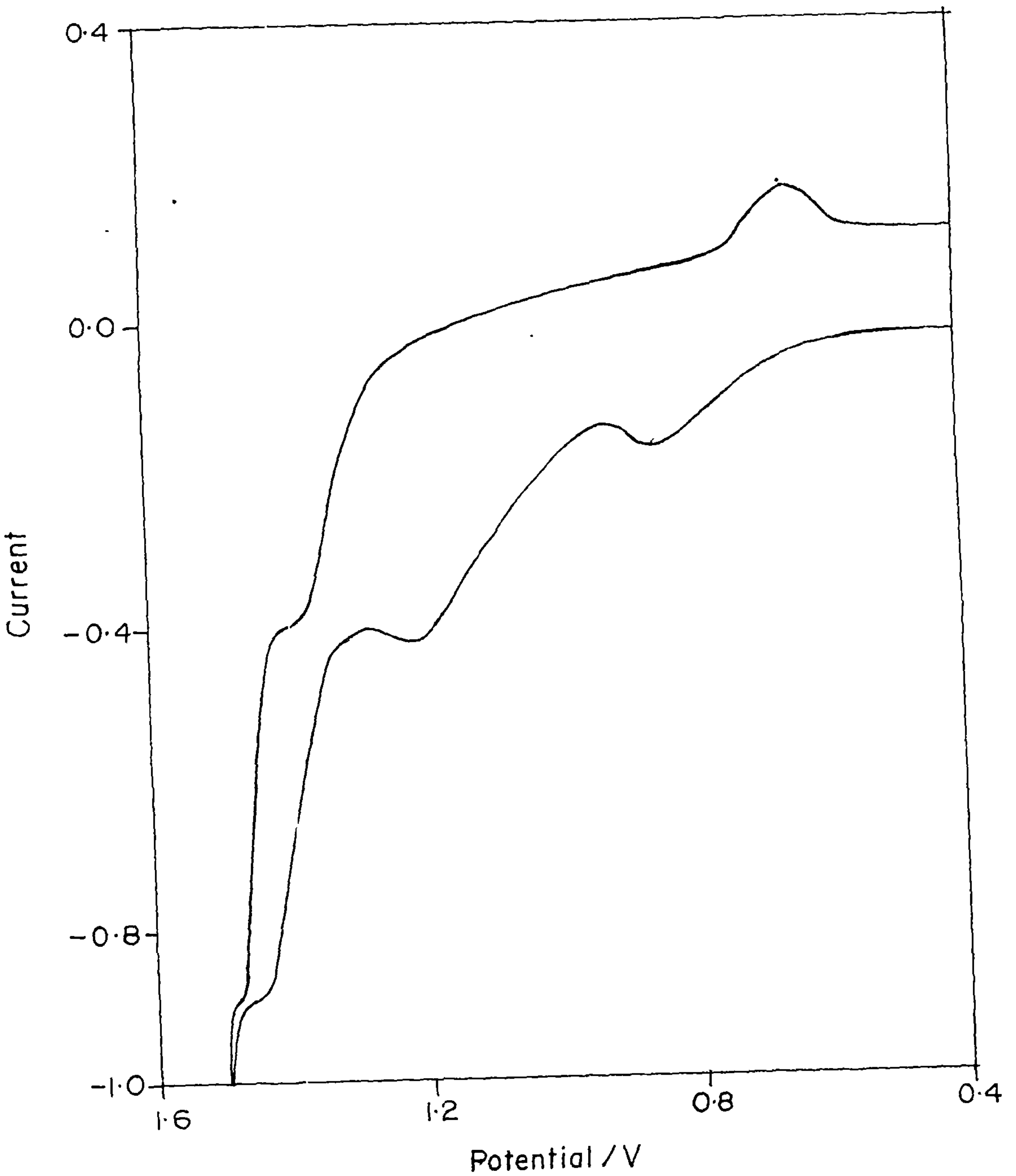

Fig.4.2.4. Cyclic voltammogram of Mn[TpyPP] in CH_2Cl_2 containing 0.1M TBAP at room temperature. Scan rate 0.01 V/s.

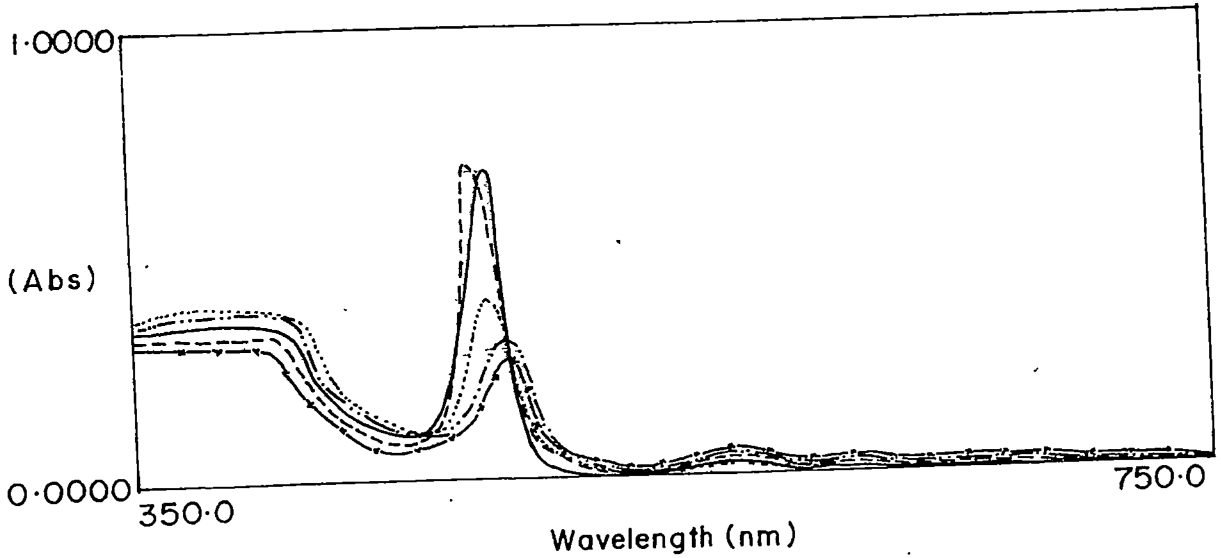

Figure.4.3.1..UV-visible absorption spectrum of Mn[T(2,5-$(OCH_3)_2$)PP] in CH_2Cl_2 oxidized with(____)$SbCl_5$ at room temperature, (....), and (----) reduced with diethyl amine
.eth.

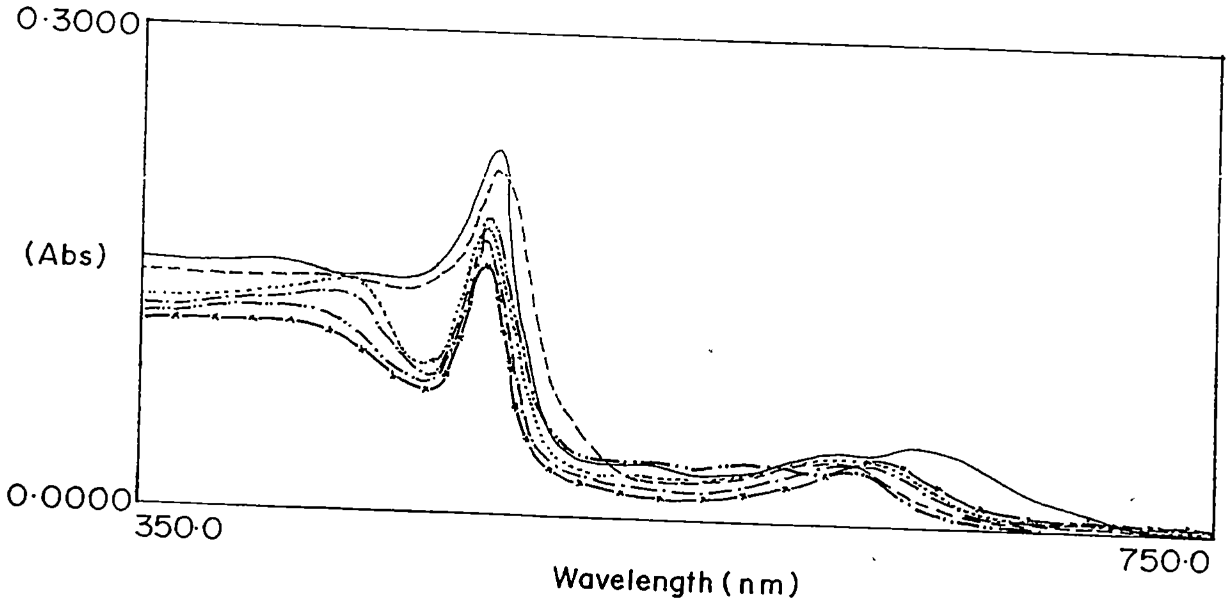

Figure.4.3.2..UV-visible absorption spectrum of Mn[T(p-OH)PP]in CH_2Cl_2 oxidized with(____)$SbCl_5$ at room temperature, (....), ... and (----) reduced with diethyl amine

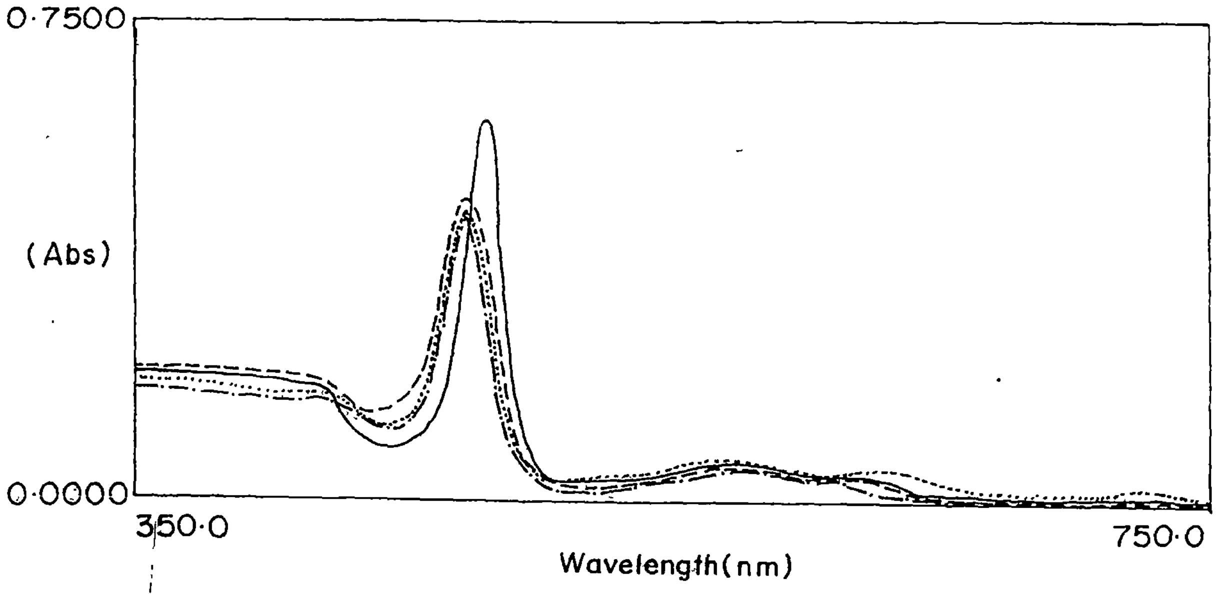

Figure.4.3.3..UV-visible absorption spectrum of Mn[T(o-NO_2)PP] in CH_2Cl_2 oxidized with(____)$SbCl_5$ at room temperature, (....), ... and (----) reduced with diethyl amine

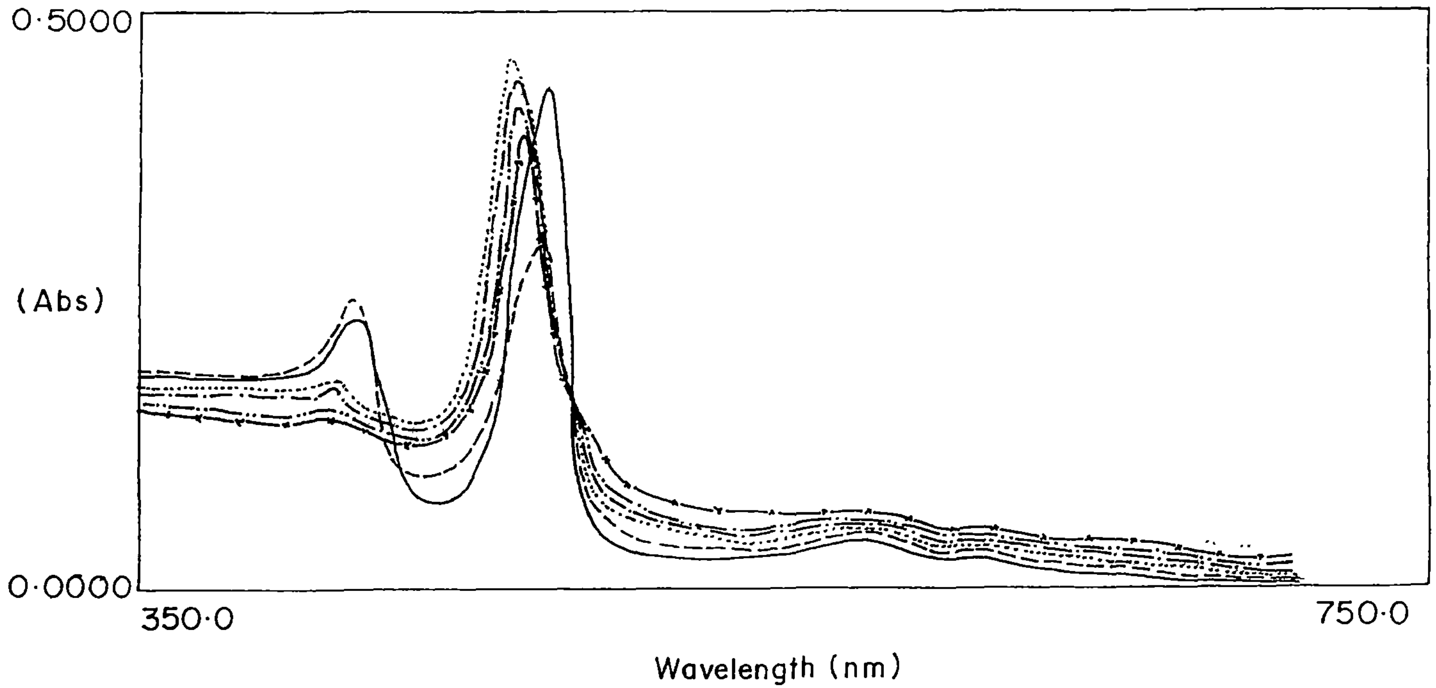

Figure.4.3.4. UV-visible absorption spectrum of Mn[TpyP] in CH_2Cl_2 oxidized with(____)$SbCl_5$ at room temperature, (....), ... and (----) reduced with diethyl amine

Table: **4.2** **Cyclic voltammetric data for Cadmium and Copper porphyrins at room temperature**

Solvent : Dichloromethane
Supporting electrolyte : TBAP
Concentration : 10^{-3}M
Reference electrode : Ag/AgCl

System/	Scan Rate (V/s)	Epa(1) V	Epa(2) V	Epa (3) V	Epc(1) V	Epc(2) V	Epc (3) V	ΔE(1) V	ΔE(2) V	ΔE (3) V	$E_{1/2}$(1) V	$E_{1/2}$(2) V	$E_{1/2}$ (3) V
Cd[T(2,5–(OCH$_3$)$_2$)PP]	0.06	1.0852	1.2791	----	1.012	1.1642	----	0.0732	0.1149	----	1.0486	1.2216	----
Cd[T(o-NO$_2$)PP	0.05	0.7149	1.5324	----	0.6027	0.9972	----	0.1122	0.5352	-----	0.6588	1.2648	----
Cu[T(2,5–(OCH$_3$)$_2$)PP]	0.02	0.638	0.910	1.243	0.5346	0.8098	-----	0.1034	0.1002	-----	0.863	0.8599	---
Cu[T(o-NO$_2$)PP	0.05	0.7702	1.2145	----	0.6607	1.0332	-----	0.1095	0.1813	-----	0.7154	1.1238	----

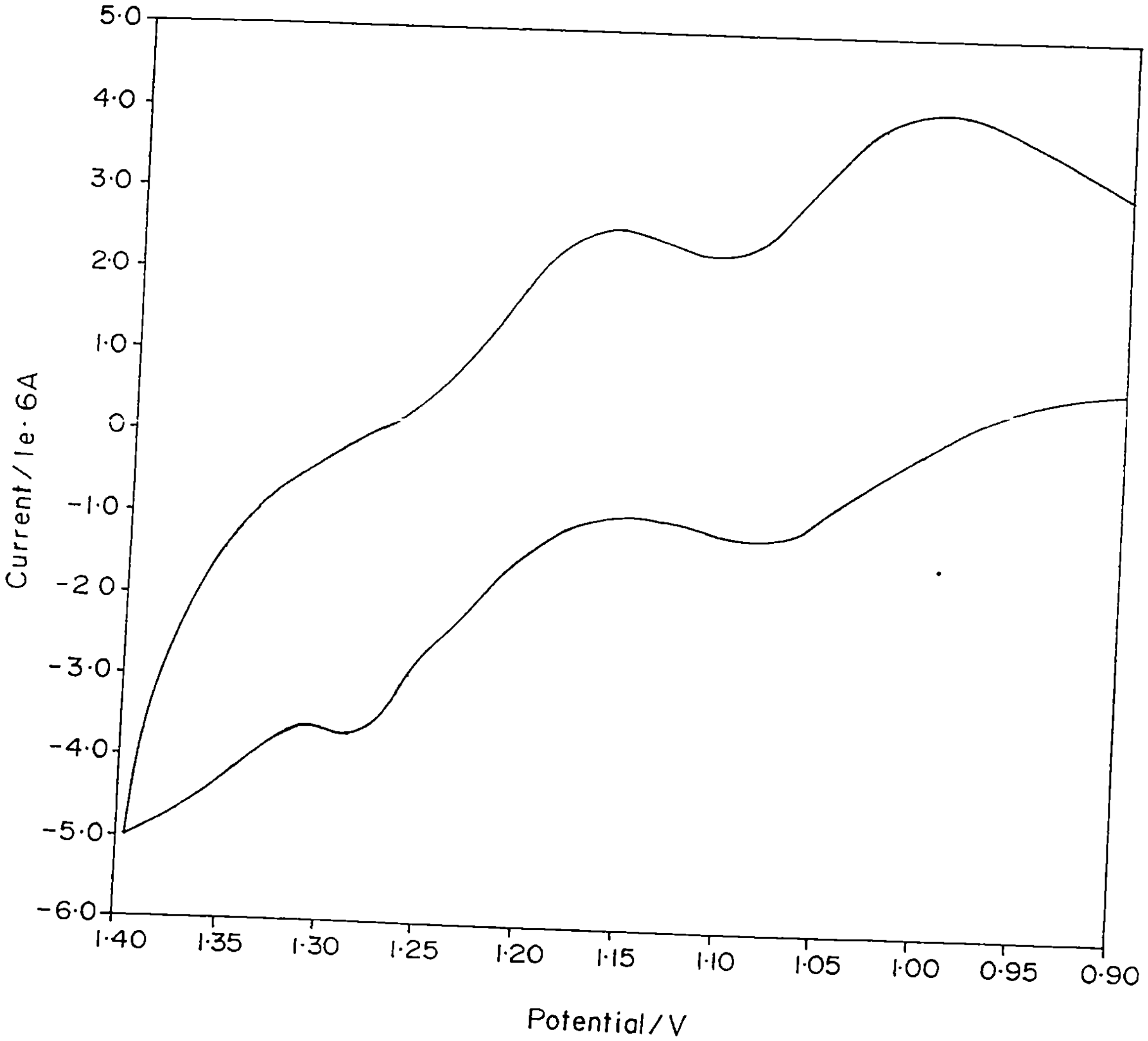

Fig.4.5.1. Cyclic voltammogram of Cd[T(2,5-$(OCH_3)_2$)PP] in CH2Cl2 containing 0.1M TBAP at room temperature Scan rate 0.06V/s

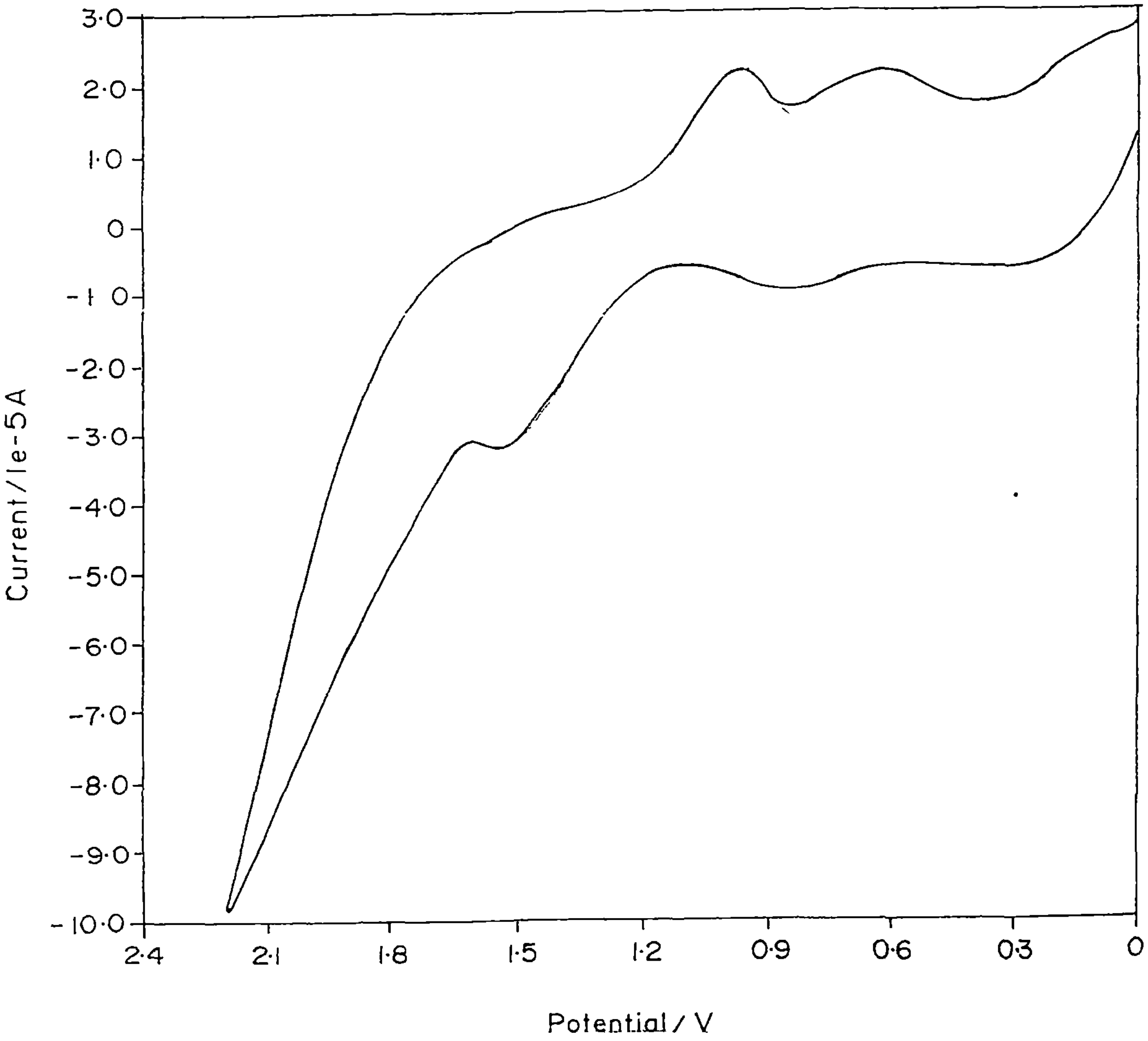

Fig.4.5.2. Cyclic voltammogram of Cd[T(*o*-NO_2)PP] in CH_2Cl_2 containing 0.1M TBAP at room temperature. Scan rate 0.05 V/s.

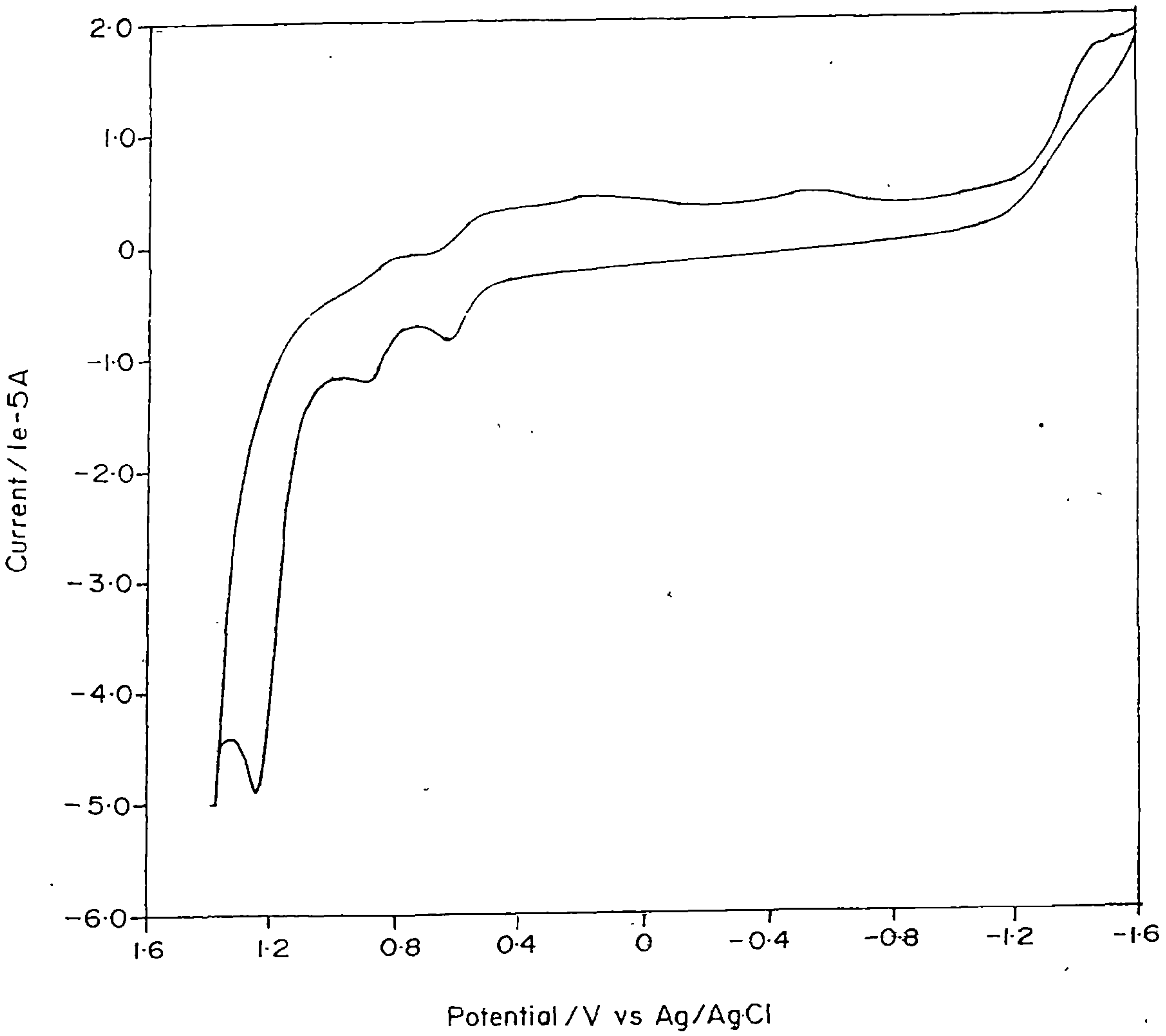

Fig.4.5.3. Cyclic voltammogram of Cu[T(2,5-$(OCH_3)_2$)PP] in CH_2Cl_2 containing 0.1M TBAP at room temperature. Scan rate 0.02 V/s

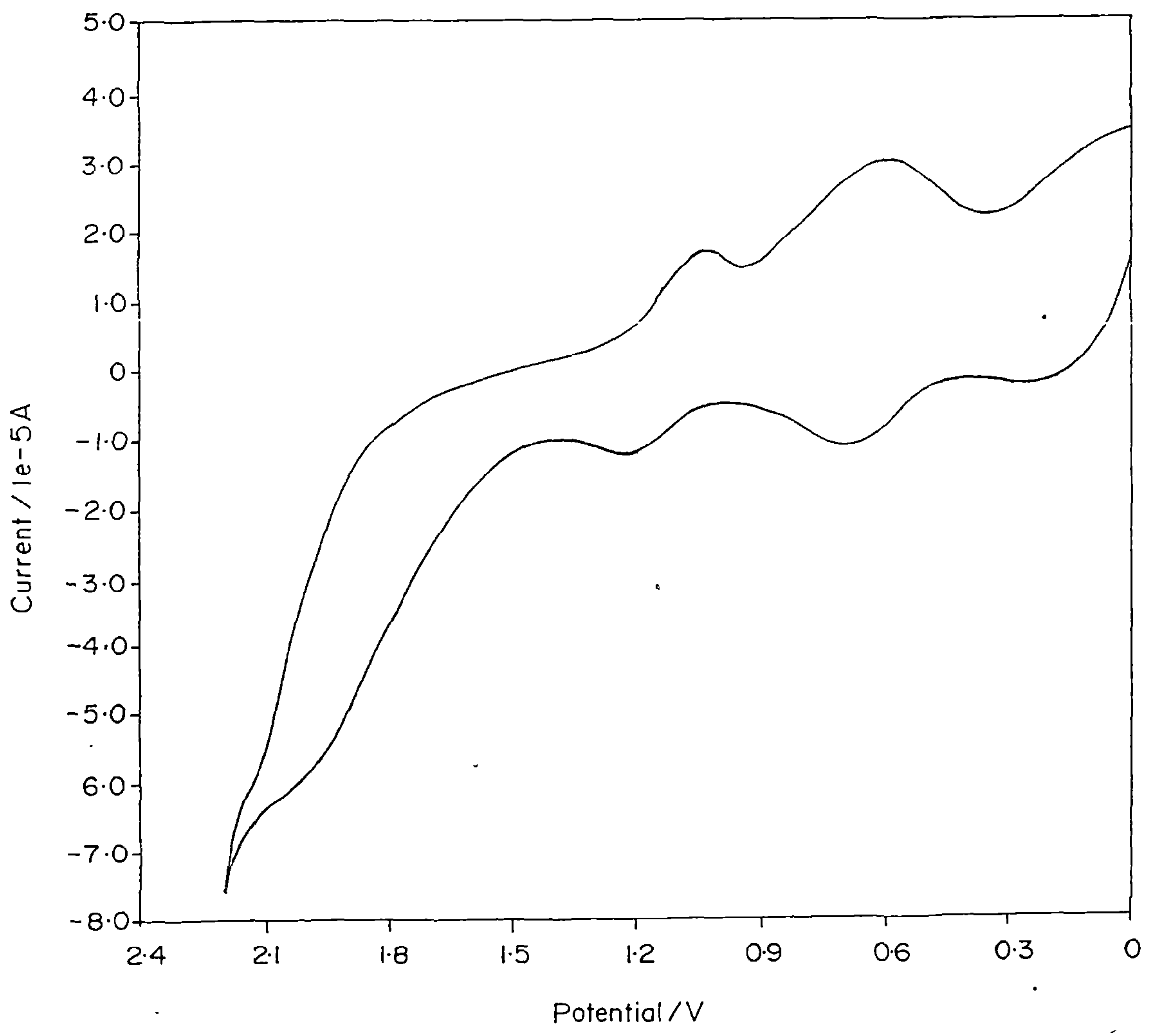

Fig.4.5.4. Cyclic voltammogram of Cu[T(*o*-NO_2)PP] in CH_2Cl_2 containing 0.1M TBAP at room temperature. Scan rate 0.05 V/s.

REFERENCES

1. C. L. Hill and B. C. Schardt, *J. Am. Chem. Soc* ., **102,** 6375 (1980)
2. J. T. Groves, W. J. Kruper, and R. C. Haushalter., *J. Am. Chem. Soc.*, **102**, 6377, (1980)
3. B. C. Schardt, F. T. Hoolander and C. L. Hill., *J. Am. Chem. Soc.*, **104**, 3964 (1982)
4. C. L. Hill and J. A. Smegal, *New. J. Chem.*, **6,** 287 (1982)
5. J. A. Smegal, B. C. Schardt, and C. L. Hill, *J. Am. Chem. Soc.*, **105**, 3510 (1983)
6. J. A. Smegal and C. L. Hill, *J. Am. Chem. Soc.*, **105**, 3515 (1983)
7. J. T. Groves and M. K. Stern., *J. Am. Chem. Soc.*, **110**, 8628 (1988)
8. G. R. Friederman, M. Halma, K. D. de F. Castro, F. L. Benedito, F. G. Doro, S. M. Drechsel, A. S. Mangrich, M. D. D. Assis and S. Nakagaki., *Applied Cata.A Gen.*,**308**, 172 (2006)
9. D. M. Gold, M. Kumar and P. Neta, *J. Phys. Chem.*, **96**, 9576 (1992)

10. G. Simonneaux, V. Schunemann, C. Morice, L. Carel, L. Toupet, H. Winkler, A. X. Trautwein, F. A. Walker., *J. Am. Chem. Soc.*, **122**, 4366 (2000)

11. A. Ghosh, I. Halvorsen, H. J. Nilsen, E. Steene, T. Wondimagegn, R. Lie, E. VanCaemelbecke, N. Guo, Z. Ou and K. M. Kaddish, *J. Phys. Chem.B*, **105,** 8120(2001)

12. A. Bettelhein, B. A. White, S. A. Raybuck and R. W. Murray., *Inorg.Chem.*, **26,** 1009(1987)

13. R. Harada, H. Okawa and T. Kojima, *Inorg.Chim.Acta.*, **538**, 489 (2005)

CHAPTER 5

ELECTRON PARAMAGNETIC RESONANCE(EPR) OF SOME SUBSTITUTED VANADYL MESO-TETRAPHENYL PORPHYRINS OXIDIZED WITH $SbCl_5$

5.1. INTRODUCTION

Electron paramagnetic resonance (EPR) is a technique which is extensively used by chemists and other scientists to monitor the paramagnetic properties of the system they study. The basic theories of the EPR are well documented in the literature. In porphyrin chemistry EPR has been used extensively and exhaustive literatures are available. In view of this we simply present here a very brief and selective discussion on paramagnetic resonance theory

In a metalloporphyrin one or more unpaired electrons may exist on the central metal atom. Also one or more unpaired electrons may be generated on the π-ligand system or on the central metal atom or in both. Such unpaired electrons will give EPR spectra and will give rise to EPR spectra. The features of EPR spectra are dependent on the number of unpaired electrons and its environment.

5.2. SOME BASIC PRINCIPLES OF EPR[1-7]

5.2.1. Resonance Condition, g-value and symmetry

An unpaired electron is associated with a spin angular momentum giving rise to a magnetic moment **μ**, which is given by

$$\mu_e = g\beta\mathbf{s} \quad \text{.................................. (4.2.1)}$$

Where g is the electron g factor and is dimensionless. B is the electronic Bohr magneton (=eħ/2mc, where e = -e, charge on the electron and m = mass of the electron).

If we subject such a system to an external magnetic field **B**, the interaction between the electron magnetic moment and the external magnetic field is given by the Hamiltonian

$$\mathbf{H} = -\,\boldsymbol{\mu}.\mathbf{B} \quad \text{................................(4.2.2)}$$

From equations (4.2.1) and (4.2.2), we get

$$\mathbf{H} = g\beta_e\mathbf{B.S} \quad \text{.......................(4.2.3)}$$

If the applied magnetic field is in the Z-direction, then

$$\mathbf{H}=g\beta_eB_ZS_Z \quad \text{-----------------------------(4.2.4)}$$

Since $S_Z = \pm 1/2$, we can have two allowed orientations of spins ($M_s = \pm 1/2$) parallel or antiparallel to H_Z , Replacing the Hamiltonian H by E (Energy), then equation (4.2.4) can be written as

$$E = (\pm 1/2)\, g\beta_eB_Z \quad \text{...........................(4.2.5)}$$

Since $\Delta E = h\gamma$ ....(4.2.5)

We get

$$H\gamma = g\beta_e B_z \text{ ....}(4.2.7)$$

gives the resonance condition. The frequency of electromagnetic radiation required to induce transitions between the two spin states is given by

$$\gamma = (g\beta_e/h)\ B_z \text{ ....}(4.2.8)$$

For a magnetic field of 3500G, the absorption frequency lies in the X-band (3 cm) microwave region. The selection rule for an EPR transition is $\Delta M_s = \pm 1$, with the irradiation oscillating magnetic field being perpendicular to the external magnetic field.

One can determine the g-value, from the experimental EPR spectrum. It's value is mainly dependent on the spin and the orbital angular momentum of the unpaired electron. For a spherically symmetric system in(S-state), the orbital angular momentum is zero and the g-value is more or less equal to free-spin value g = 2.0023. For an organic free radical, the electrons are delocalized, and have very little angular momentum resulting in a small derivation from the free electron g-value. The picture is different in the case of transition metals. In a transition metal complex the orbital angular momentum of the metal electron(s) is quenched fully or partially by the ligand atoms or by other neighboring ions. This leads to a deviation from the free spin g-value.

This derivation is correlated to the spin-orbit interactions. In solid state g-value depends on the symmetry i.e. the orientation of the magnetic field to the symmetry axes of the electric field about the ion. This leads to the anisotropy in g-values. One can observe EPR signals at two g-values for a polycrystalline sample if the ligand field has an axial symmetry. For such system two types of absorptions are exhibited in the spectrum. A major absorption is observed if the external magnetic field is perpendicular to the symmetry axis (considering the symmetry axis as Z axis, then $g_x = g_y = g_\perp$) and minor absorption is observed if the applied field is parallel to the symmetry axis. Most of the metalloporphyrins have axial symmetry and we observe two g-values. If the symmetry changes, we may observe more g-values. This is what we observe in the case of orthorhombic, where three different g-values are exhibited. On the other hand the situation is different in solution. The molecules are in rapid tumbling motion and averages out to a single g-value. It is also to be noted that the g-value depends on the oxidation state of the metal ion.

5.2.3. ZERO FIELD SPLITTING AND FINE STRUCTURE

For a system having a total spin S>1/2 i.e. having more than one unpaired electron, we often see some 2S features in the spectra especially in the oriented system. This structure is known as fine structure. This fine structure is due to the interaction of the individual magnetic moments (due to spin) with the magnetic fields generated by other electrons. This interaction exists even in the absence of the external magnetic field. This phenomenon is called the zero field splitting. Thus, the fine structure reflects a splitting of the (2S+1) levels in the absence of the external magnetic field. Obviously, zero field splitting lead $\Delta M_S = 1$ transitions to occur at different values of the applied field for a particular microwave frequency. The EPR spectrum of $\Delta M_S = 1$ transitions is sometimes anisotropic and one can determine the zero field splitting from its analysis. Zero field splitting observed for transition metal ions if there are some distortions in the cubic symmetry. The effect of zero field splitting for $\Delta M_S = 1$ and $\Delta M_S = 3/2$ is shown below (fig.5.2.1) . From the EPR measurements of the zero field splitting one can also approximately calculate the average distance between two unpaired electrons of a triplet state (organic triplet state molecule).

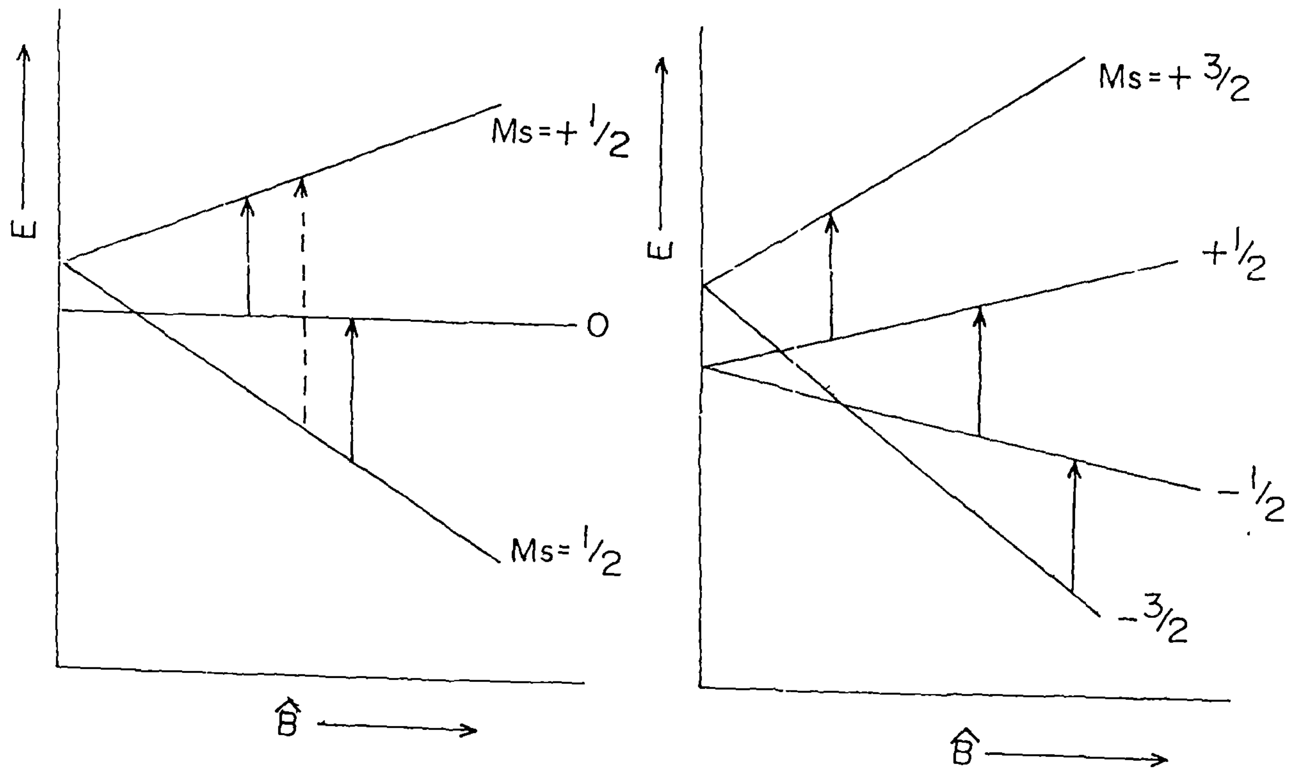

Fig.5.2.1. Effect of zero field splitting, Energy levels
A triplet state (*ii*) a quartet state for of an axially symmetric system
Arrow (→) indicates $\Delta M_s = 1$ and dotted line (┈┈┈➤) indicates $\Delta M_s = 2$

5.3. HYPERFINE INTERACTION

One of the main objectives of the EPR measurements is to obtain the hyperfine splittings, and to analyze and interpret it. The hyperfine interactions originate from the interaction between the magnetic moment of the unpaired electron spin and the magnetic moment of the nuclei present in the system. There are two types of such interaction viz. (a) Fermi contact interaction and (b) Dipolar interaction.

(a) FERMI CONTACT INTERACTION

This interaction occurs due to the non vanishing electron spin density on the surface of the nucleus or in the S-orbital of the atom. This is so because p, d, f orbitals have nodes at the nucleus. In the case of the organic π-radical the hyperfine interaction of occurs due to σ –π spin polarization mechanism. Similarly, a contact interaction occurs involving a transition metal ion. In both cases some electron spin density should exist in the S-orbital of the atom. This spin polarization mechanism is explained elsewhere in the literature. However, the better explanation may be given if we invoke Realistic quantum mechanics. The hyperfine coupling constants are observed to be much large for transition metal ions than those for organic free radicals.

(b) THE DIPOLAR INTERACTION

This interaction is similar to the classical dipolar interaction between two bar magnets. In solution this interaction averages out to zero due to rapid tumbling motions of the molecules. We normally observed this interaction only in the solid state. Therefore, it depends on the orientation of both the magnetic moments ie. Electrons spin moment and the nuclear magnetic moment with respect to the applied magnetic moment. Thus, it is anisotropic. This interaction becomes more complicated in the case of transition metal ion due to spin-orbit coupling which is also dependent on the symmetry of the molecule.

5.4. LINE SHAPE AND RELAXATOPM

To obtain information out of EPR spectra one has to study the line shape /line widths. Shape of the EPR lines depends greatly on the sin relaxation time. We observe EPR observe EPR absorption line due to population difference between the two spin states (large population in the lower energy spin state) at thermal equilibrium,. This condition is maintained by spin relaxation. Therefore, it is obvious that the spin states have finite life time. Thus, the line widths of an EPR spectrum are inversely proportional to the relaxation line. In this case the relaxation undergo without emission of radiation. The relaxation process through two mechanisms via spin-lattice relaxation and spin-spin relaxation. Spin-lattice relaxation involves spin-orbit coupling. Strong spin-orbit coupling results in a short spin-lattice relaxation time (T_1) giving broad lines or sometimes too broad for detection (say at room temperature). On lowering the temperature (liquid nitrogen, liquid helium) the spin lattice relaxation time (T_1) *increases and we observe* EPR *spectra. Obviously, at lower* temperature the lower energy spin state population increases and we observe better EPR spectra. One observes sharper EPR spectra for free radicals even at room temperature. This is because in free radicals, the spin-orbit coupling is negligible and gives rise to longer spin-lattice relaxation time. Thus, free radicals exhibit narrower line widths

Spin-spin relaxation occurs due to the intermolecular interactions. A particular molecule having an unpaired electron will have spin moment which will be affected by the local field generated by the neighboring spins. These local fields produce fluctuation in the actual external magnetic applied (B_o). Therefore, this particular spin will experience a field equal to $B_o + B_{local}$. Further, it also induces transitions within the system. Obviously, spin-spin relaxation is concentration dependant. Thus, spin-spin relaxation time (T_2) decreases with increase in concentration and vive versa. Therefore, for a strong paramagnetic sample, sharper EPR lines will be obtained on dilution.

Besides, these two processes mentioned above there are other factors that contribute to the EPR line shape.

Normally, one encounters of line shapes via, Lorentzian and Gaussian. In solution spectra one commonly encounters Lorentzian line shape, which is given by

$$f(w) = [(1/\hbar)(1/T_2)]/[(1/T_2)^2/(w_0 - w)]^2 \ldots\ldots\ldots\ldots (4.4.1)$$

where w_0 is the angular frequency corresponding to the centre of the line and w is the angular frequency of normal additional field B_1

In solid spectra one generally observe Gaussian line shape which is given by

$$f(w) = T_2(2\hbar)^{-1/2}\exp[-1/2\ T_2^2(w_o-w)^2] \ldots\ldots\ldots\ldots\ldots\ldots\ldots (4.4.2)$$

5.5. SPIN HAMILTONIAN

One can write the spin Hamiltonian for Hydrogen atom easily as

$$H = g\beta BS_z - g_N\beta_N BI_z + a.\mathbf{S}.\mathbf{I} \ldots\ldots\ldots\ldots\ldots\ldots\ldots\ldots\ldots\ldots\ldots (4.5.1)$$

The third term in the equation (4.5.1) tells that it is isotropic hyperfine coupling, but does not indicate anything about the mechanism of the coupling. Therefore, one has to formulate proper spin Hamiltonian and obtain the values of these parameters from the experimental EPR spectra and fit them into the spin Hamiltonian. In transition metal ions, spin-orbit coupling complicates the EPR spectra. In the spin Hamiltonian terms like **S.B, L.B, S.I.S.I, L.I, S.L and $S_1.S_2$** occur.(where **S** = electron spin, **I** = nuclear spin **B**= external magnetic filed, **L** = orbital angular momentum and **S_1** and **S_2** are the spins electrons 1 and 2 respectively). To interpret the EPR spectra in terms of these interactions is quite different and not straight forward. The effect of the spin-orbit coupling is included in the g-values ($g_x = g_y = g_z$) and the hyperfine coupling A_x, A_y, A_z. These values can be obtained from the experimental EPR spectra and then fit into the spin Hamiltonian. One can compute the spin Hamiltonian parameters by proper choice of wave function. It is to be noted that the Hamiltonian has to be defined with respect to the co-ordinates of g tensor and A tensor in which they are diagonal.

5.6. METALLOPORPHYRINS WITH PARAMAGNETIC METAL ATOM UNPAIRED ELECTRON ON THE LIGAND

In general there are two types of porphyrin ligands: (i) OEP-type (OEP = octa ethyl porphyrin) and (ii) TPP type (TPP = meso tetraphenyl porphyrin)[8-13].

(i) OEP type: The porphyrin ligands which do not have any substituents in the meso positions. Typical examples are octaethyl porphyrin, Etio porphyrin, proto porphyrin and many other naturally occurring porphyrins.

(ii) TPP type: The porphyrin ligands which have alky or aryl substituents into meso positions. Typical example is mesotetraphenyl porphyrin. etc.

In a metalloporphyrin having D_4h symmetry, the highest occupied pi molecular orbits are very close lying, with symmetry labels a_1u and a_2u. The energy difference between these two molecular orbitals is of the order of 0.5ev or less. Therefore, their relative ordering is quite sensitive to the central metal ion. However, it has been normally observed that for metalloporphyrin radical cations belonging to OEP type the HOMO (Highest occupied molecular orbital) have a_1u ground state. On the other hand that of the TPP type has a_2u ground state. It is to be noted that these generalization is not rigid and in some case the ground state of the pi radical changes from a_1u to a_2u on changing the axial ligand. On the whole the above generalization holds fairly well for a large number of metalloporphyrin,

5.7. EPR OF SOME SUBSTITUTED VANADYL meso-TETRAPHENYL PORPHYRINS OXIDIZED WITH $SbCl_5$

5.7.1. RESULTS

(i) VO[T(*o*-NO_2)PP]

Oxidation of VO[T(*o*-NO_2)PP] with $SbCl_5$ follows exactly in the same manner to that of the VOTPP oxidation. Addition of 1.8ml of 0.1M $SbCl_5$ to 0.2ml of 10^{-3}M VO[T(*o*-NO_2)PP] gives rise to the spectrum(fig.5.7.1(i)). Further addition of $SbCl_5$ leads to triplet state.

(ii) VO[T(2,5-$(OCH_3)_2$)PP]

Addition of 2.6ml of 0.1M $SbCl_5$ to 0.2ml of 10^{-3}M VO[T(2,5-$(OCH_3)_2$)PP] give the spectrum(fig.5.7.1(ii)A). Further addition of $SbCl_5$ leads to triplet (fig.5.7.1(ii)B). This leads to a triplet state.

(iii) VO[TpyP]

Addition of 1.2ml of 0.1M $SbCl_5$ to 0.2ml of 10^{-3}M VO[TpyP] exhibits the spectrum(fig.5.7.1(iii)A). Further addition of $SbCl_5$ yield the spectrum (fig.5.7.1(iii)B).

(iv) VO[T(*p*-OH)PP]

Oxidation of VO[T(*p*-OH)PP] with $SbCl_5$ gives rise to the spectrum(fig.5.7.1(iv)A). Further addition of $SbCl_5$ give rise to spectrum (fig.5.7.1(iv)B) and the spectrum (fig.5.7.1(iv)C). EPR parameters are summarizing in the table 5.1. The formation of mono cations is further supplemented by IR spectra[18-19]. In all cases an additional band at 1275 cm^{-1} are observed (fig.5.7.(v)). Further, during the oxidation with $SbCl_5$, demetallation does not take place. This is checked by taking UV-Vis spectra after quenching the solutions containing mono cations and the $SbCl_5$ with diethyl amine. (fig.5.7.(vi) A, B, C, and D).

5.7.2 DISCUSSION

Except for the VO[T(*p*-OH)PP] other three vanadyl porphyrins undergo oxidation with $SbCl_5$ in the same manner to that of VOTPP oxidation[14-17]. In case of VO[T(*o*-NO_2)PP]

It clearly undergoes oxidation quite similar to that of the oxidation of VOTPP. Oxidation steps can be represented as

$$\begin{tikzcd} VO[T(o\text{-}NO_2)PP] \arrow[r] & \underset{I}{VO[SbCl_4Cl\text{-}T(o\text{-}NO_2)PP]SbCl_5} \arrow[d] \\ & \underset{II}{VO[T(o\text{-}NO_2)PP^+]Cl^-} \end{tikzcd}$$

The pre oxidized form I is observable at room temperature. Further, it forms triplet state (II) on further addition of $SbCl_5$ and its spectrum is observable at a higher modulation[16]. The EPR parameters are obtained using the simulation program.

In the case of VO[T(*p*-OH)PP] formation of solids(precipitates) on further addition of $SbCl_5$ is observed. This is due to polymerization which is also observed by some earlier workers[20]. This is also evident from the CV study. The cations of these vanadyl porphyrins give two g-values indicating that the ligand field possesses an axial symmetry

5.7.3. CONCLUSION

From the EPR study of the oxidation of VO[T(2,5-$(OCH_3)_2$)PP], VO[T(*p*-OH)PP], VO[T(*o*-NO_2)PP], and VO[TpyP] with $SbCl_5$ following observations are made

i) Except VO[T(*p*-OH)PP] all three vanadyl porphyrins undergo oxidation with $SbCl_5$ generating radical cations in the same process to that of the oxidation of VOTPP.

ii) The pre-oxidized species are also observable at room temperature. The triplet state spectra are observable at higher modulation even at room temperature.

iii) The inter-electronic distances ranging between 3.629A° – 3.601A° are observed which points to a_2u ground state.

iv) VO[T(*p*-OH)PP] polymerizes on oxidation.

Table.5.1: ESR spectrum at Room Temperature

Metalloporphyrin	Inter electron distance R(A^0)	Unoxidized g value	Oxidized g value		Oxidized A(G) Value	
			$g_{\parallel}$	$g_{\perp}$	$A_{\parallel}$	$A_{\perp}$
VO[T(2,5-(OCH$_3$)$_2$)PP]	3.629	1.984	1.932	1.971	2.349	1.768
VO[T(p-OH)PP]	3.621	1.999	1.920	1.989	3.280	1.949
VO[T(o-NO$_2$ PP]	3.612	1.975	1.928	1.969	3.620	1.940
VO[TpyP])	3.601	1.987	1.911	1.963	3.009	2.422

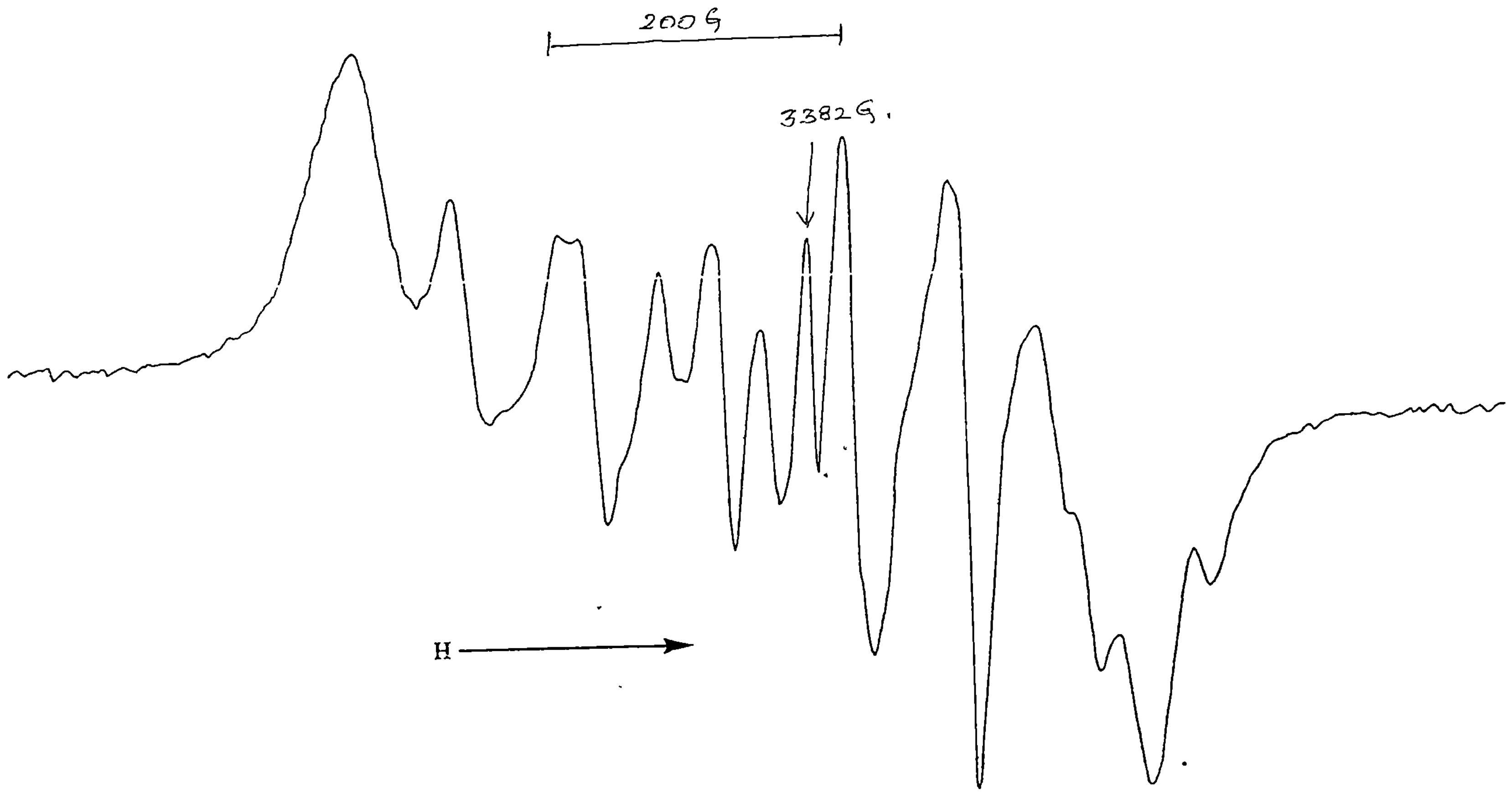

Fig. 5.7.1 (i) Room temperature X – band EPR spectra of VO [T(o-NO_2)PP] in Dichloromathene oxidized with $SbCl_5$

Experimental conditions:

Modulation Frequency = 100 KHz
Microwave power = 2 mW
Microwave frequency = 9.33 GHz. Scan Hme 8 min, scan range 1600G
Modulation amplitude = 0.5 x 10G

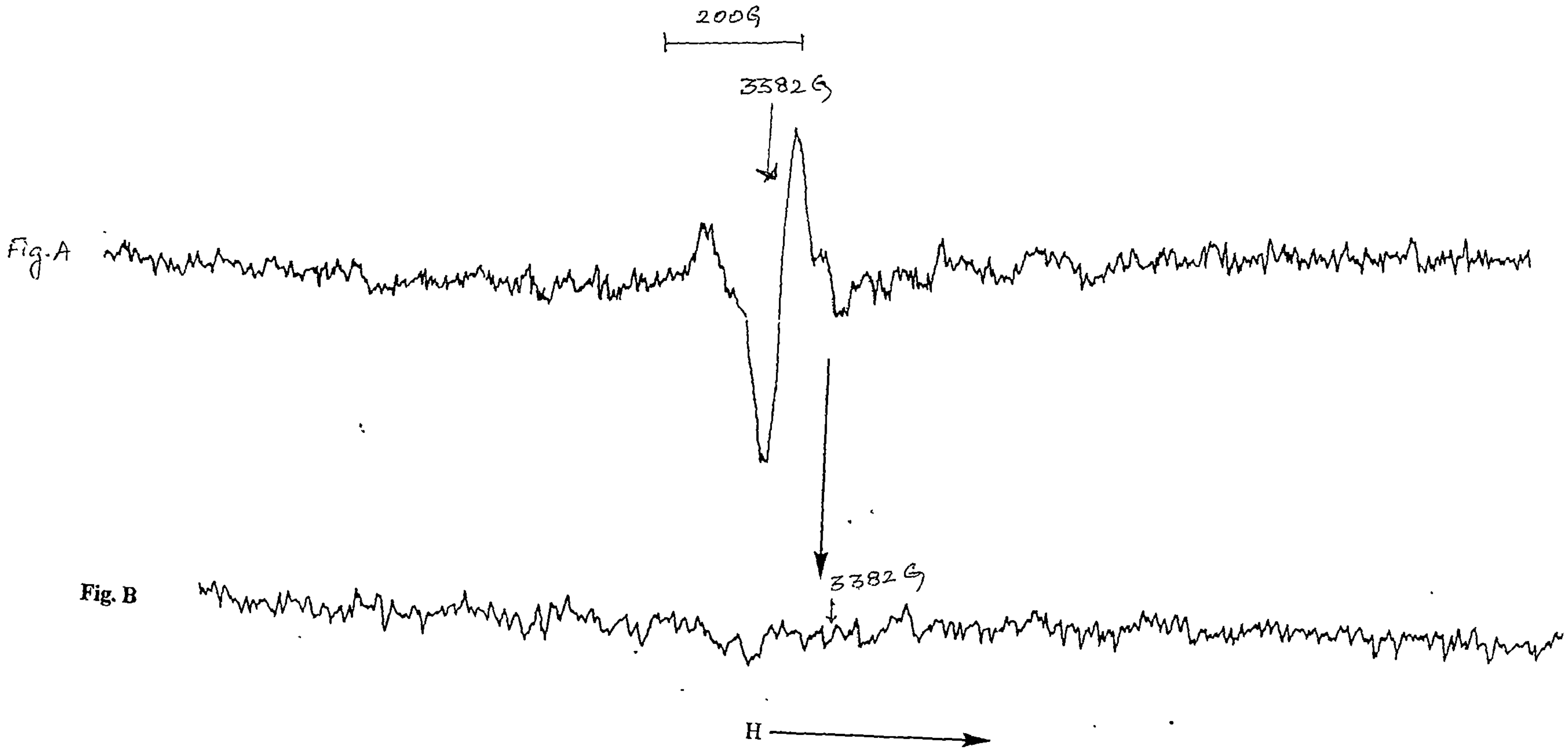

Fig. 5.7.1 (ii) Room temperature X – band EPR spectra of VO [T(2,5 – $(OCH_3)_2$)PP] in Dichloromathene oxidize with $SbCl_5$

Experimental conditions:

Modulation Frequency = 100 KHz
Microwave power = 2 mW
Fig (A) Microwave frequency = 9.31 GHz. Scan Hme 8 min, scan range 1600G
Modulation amplitude = 1.6 x 10G
Fig (B) Microwave frequency = 9.33 GHz. Scan Hme 8 min, scan range 1600G
Modulation amplitude = 1.8 x 10G

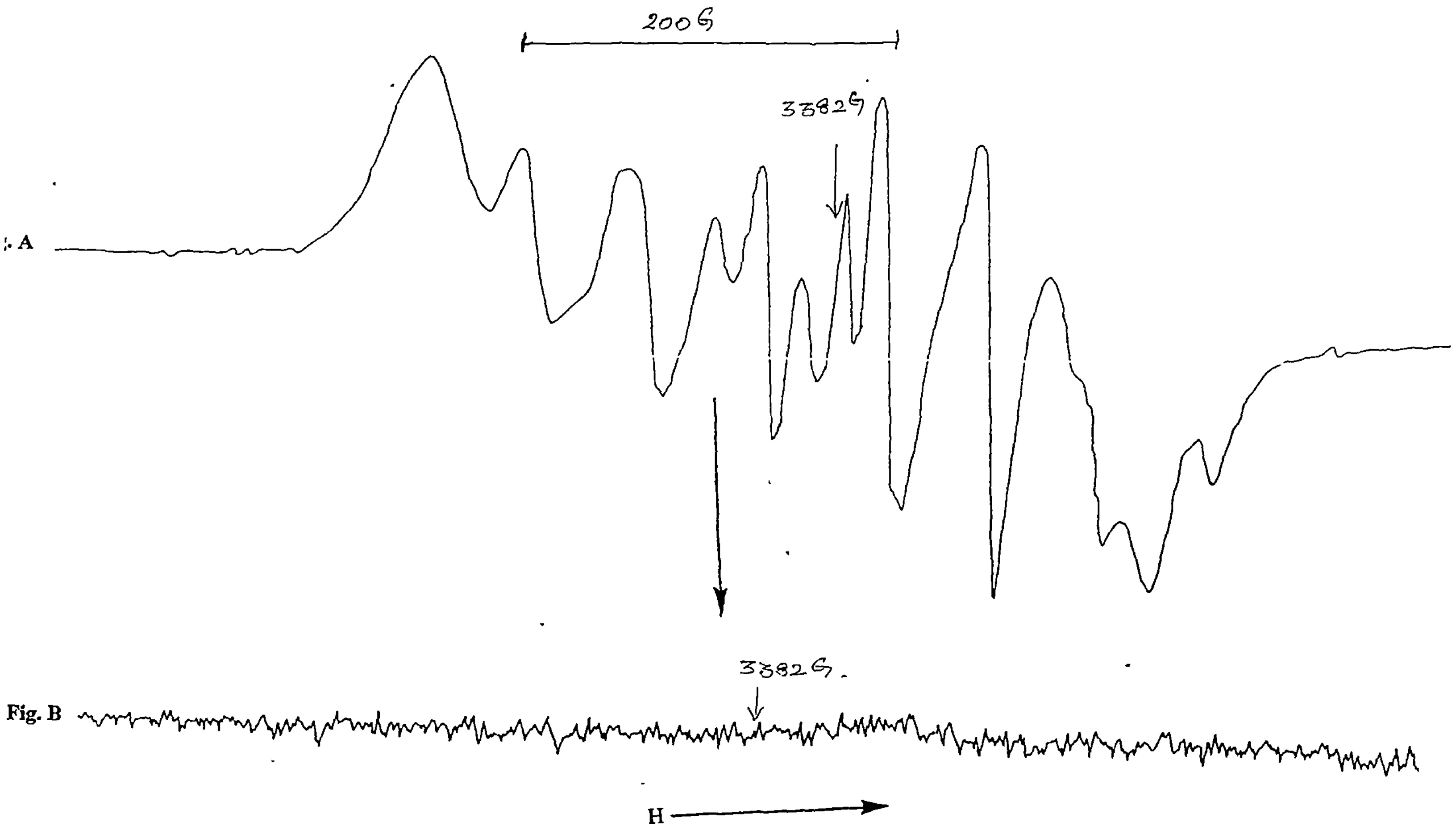

Fig. 5.7.1 (iii) Room temperature X – band EPR spectra of VO [TPyP] in Dichloromathene oxidized with $SbCl_5$

Experimental conditions:

Modulation Frequency = 100 KHz
Microwave power = 2 mW
Fig (A) Microwave frequency = 9.38 GHz. Scan Hme 8 min, scan range 1600G
Modulation amplitude = 0.5 x 10G
Fig (B) Microwave frequency = 9.4 GHz. Scan Hme 8 min, scan range 1600G
Modulation amplitude = 0.9 x 10G

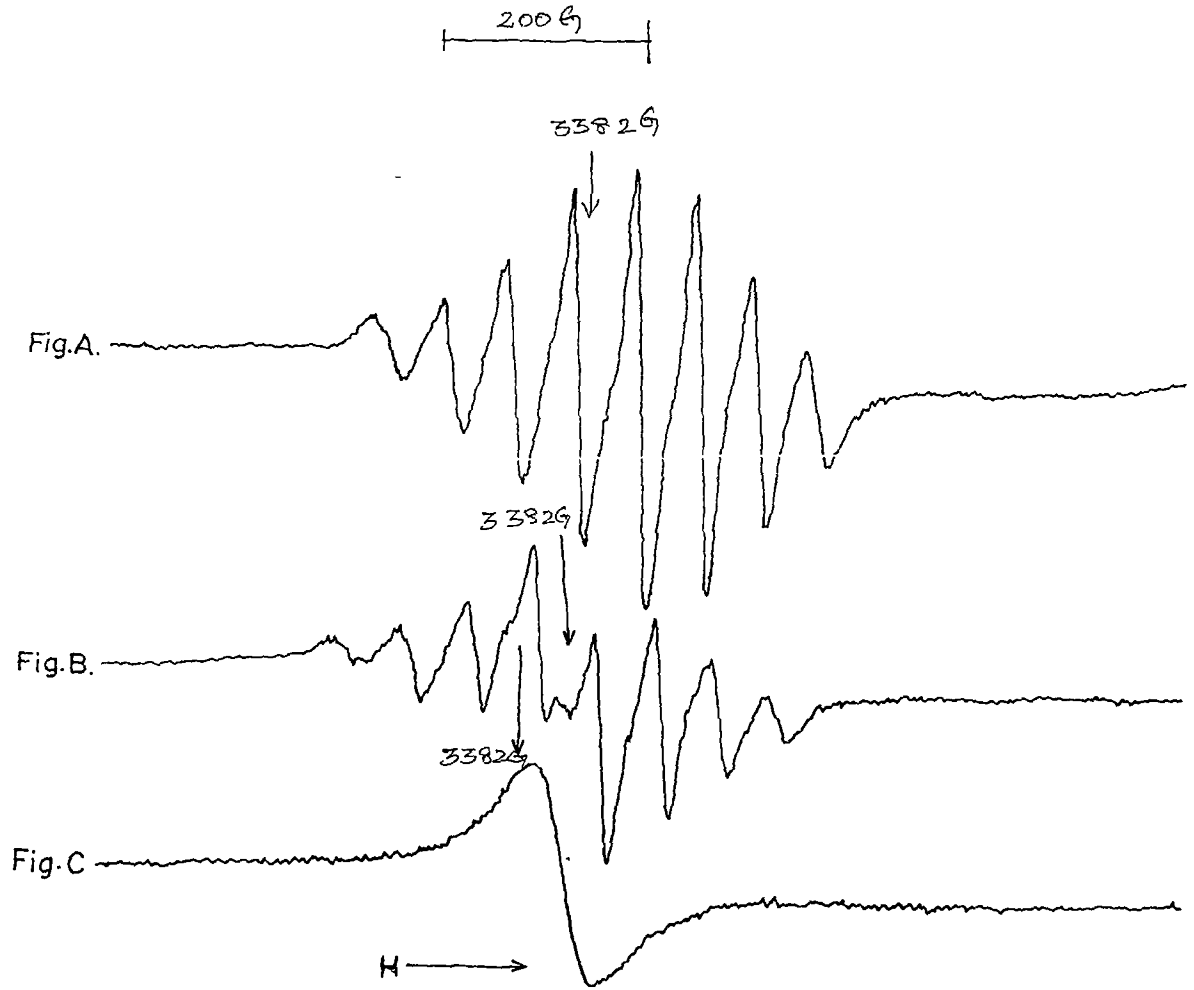

Fig. 5.7.1 (iv) Room temperature X – band EPR spectra of VO [T(p-OH)PP] in Dichloromathene oxidized with $SbCl_5$

Experimental conditions:

Modulation Frequency = 100 KHz
Microwave power = 2 mW
Fig (A) Microwave frequency = 9.31 GHz. Scan Hme 8 min, scan range 1600G
Modulation amplitude = 0.8 x 10G
Fig (B) Microwave frequency = 9.33 GHz. Scan Hme 8 min, scan range 1600G
Modulation amplitude = 1.6 x 10G

Fig (C) Microwave frequency = 9.4 GHz. Scan Hme 8 min, scan range 1600G
Modulation amplitude = 2 x 10G

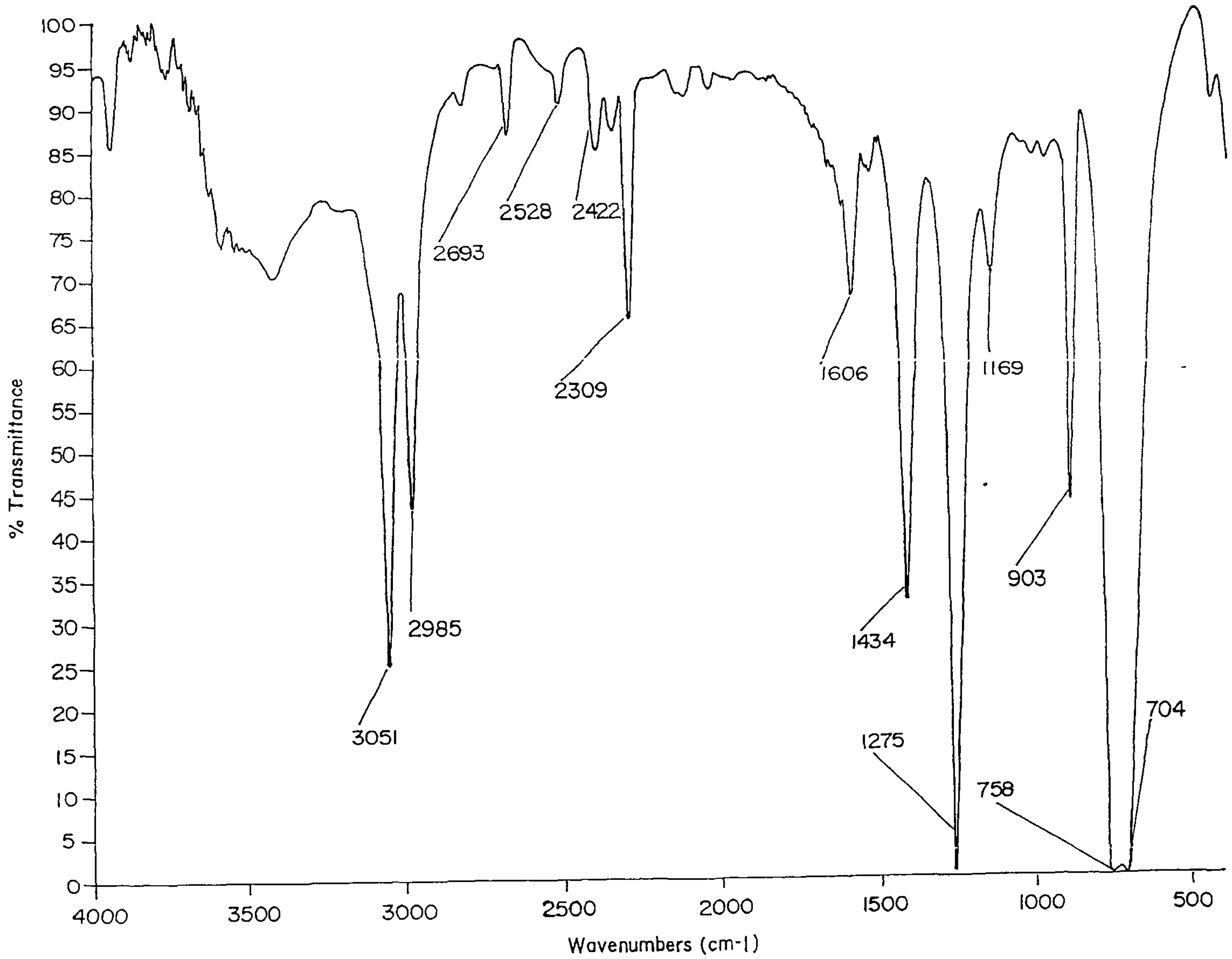

fig.5.7.(v) Infrared spectrum of of VO[T(2,5-$(OCH_3)_2$)PP] in CH_2Cl_2 oxidized with $SbCl_5$ at room temperature

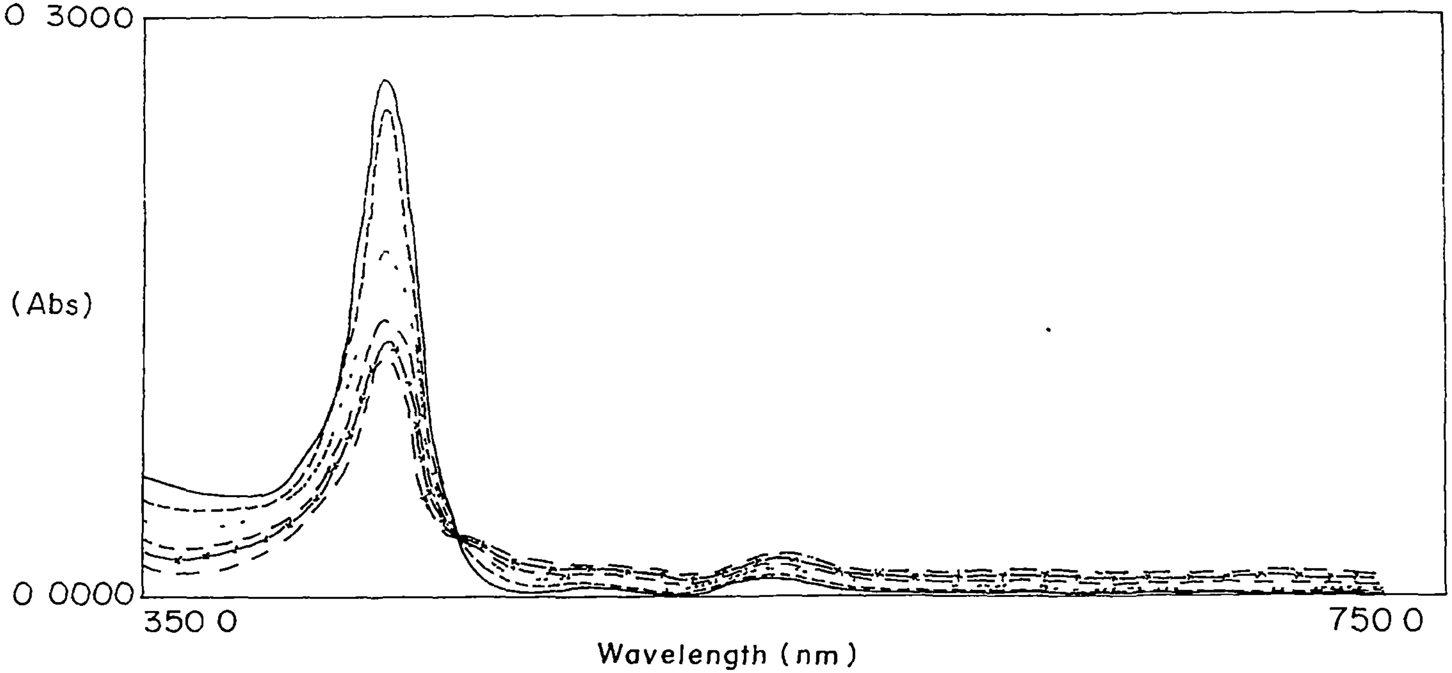

Figure.5.7.1 (vi) A..UV-visible absorption spectrum of VO[T(2,5-$(OCH_3)_2$)PP] in CH_2Cl_2 oxidized with(____)$SbCl_5$ at room temperature, (….), and (----) reduced with diethyl amine

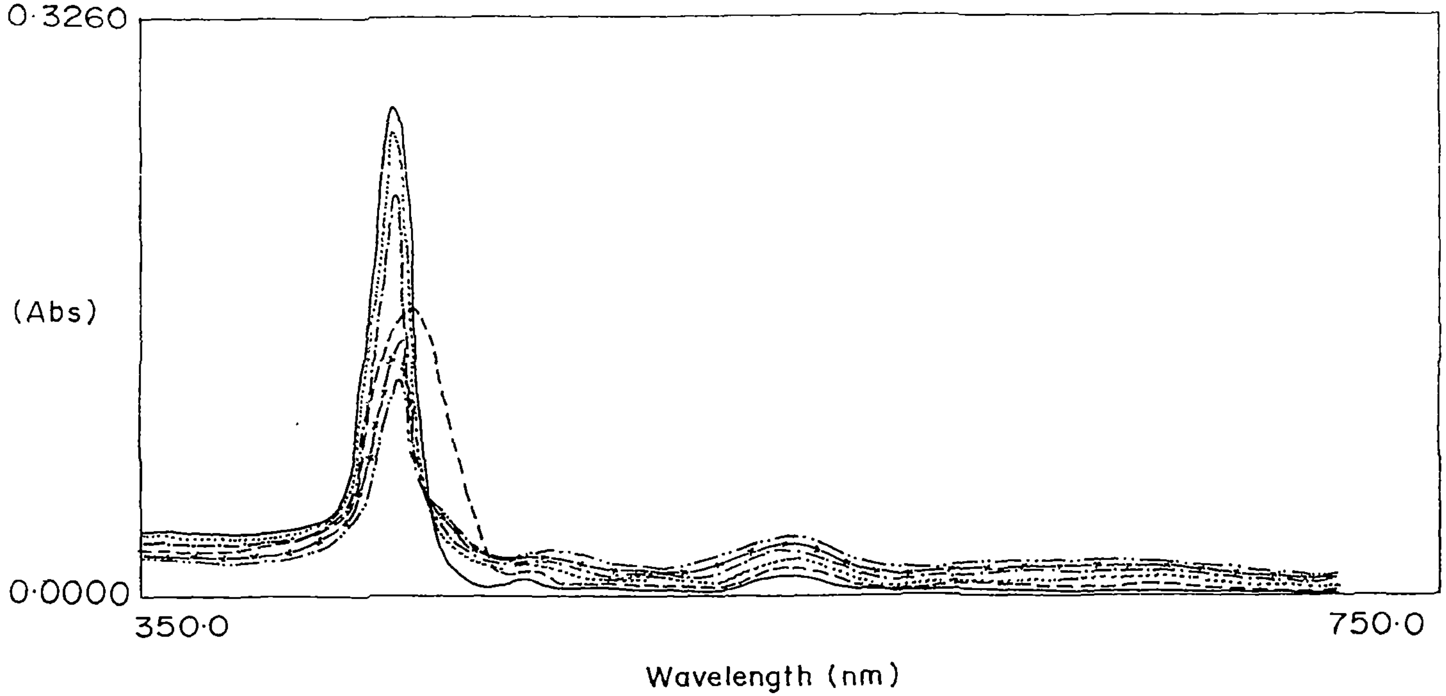

Figure.5.7.1 (vi) B..UV-visible absorption spectrum of VO[T(p-OH)PP]in CH_2Cl_2 oxidized with(____)$SbCl_5$ at room temperature, (….), … and (----) reduced with diethyl amine

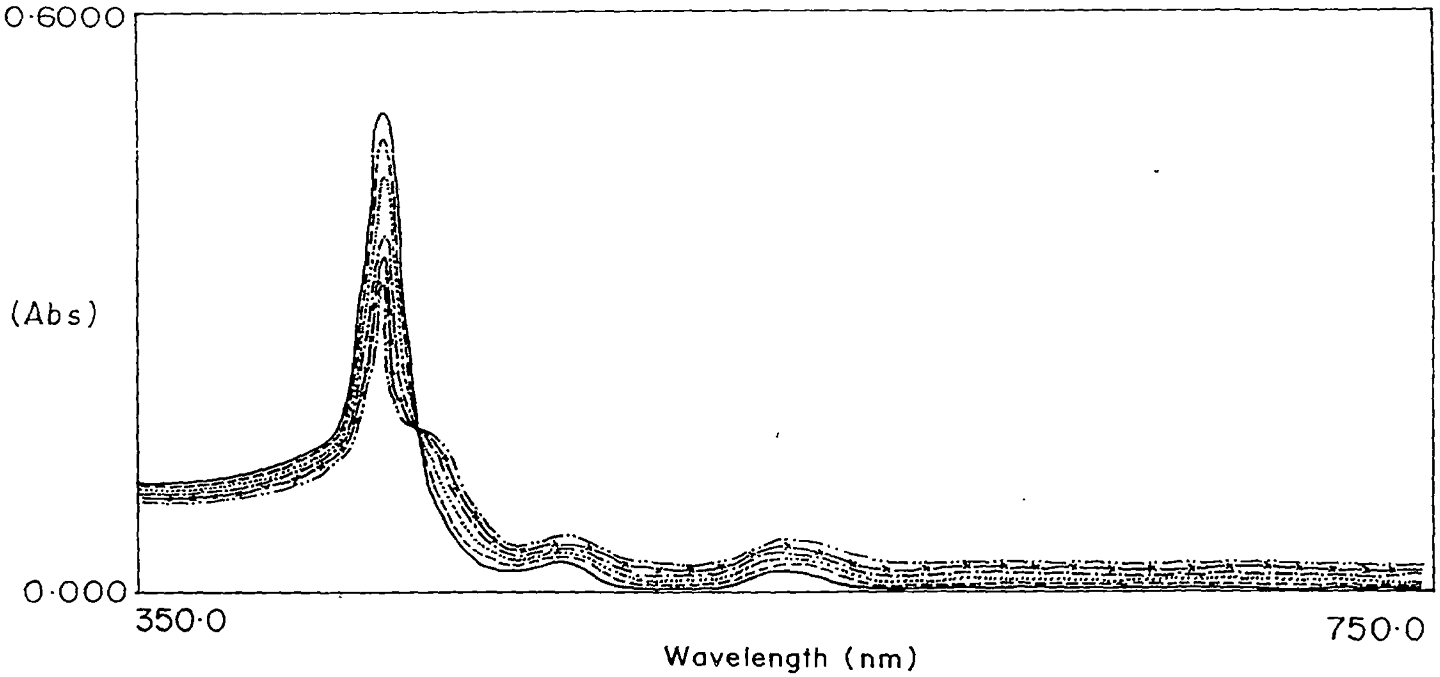

Figure.5.7.1 (vi) C..UV-visible absorption spectrum of VO[T(o-NO_2)PP] in CH_2Cl_2 oxidized with(____)$SbCl_5$ at room temperature, (….), :….. and (----) reduced with diethyl amine

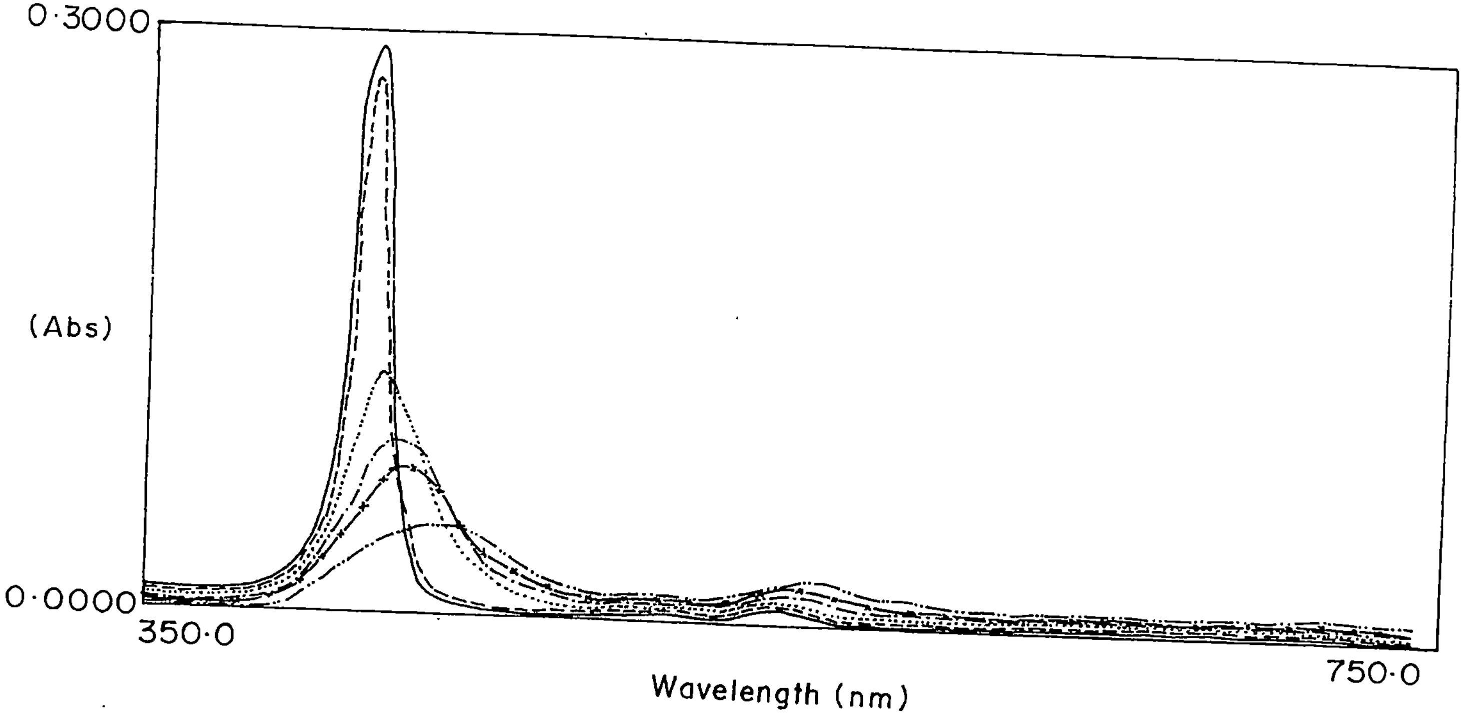

Figure.5.7.1 (vi) D..UV-visible absorption spectrum of VO[TpyP] in CH_2Cl_2 oxidized with(____)$SbCl_5$ at room temperature, (….), …… and (----) reduced with diethyl amine

REFERENCES

1. N. M. Atherton., "*Electron spin Resonance-theory and application*" Ellis Harwood limited, Sussex, England(1973)
2. J.E. Wertz and J.R.Bolton, "*Electron spin resonance-Elementary theory and Practical application*" Edition McGraw Hill New York(1972)
3. A. Carrington and A. D. McLahlen, " *Introduction to Magnetic resonance*" Harper and Row, New York(1967)
4. A. Abragan and B. Bleaney, " *Paramagnetic resonance of transition metal ions*" Oxford University press (1970)
5. B. R. McGarvey in " *Transition metal chemistry*", Vol.3, R. L. Carlin (Ed.)., Marcel Dekker, New York (1966)
6. H. M. Schwalz., J. R. Bolton and D. C. Borg(Eds.)," *Biological application of electron spin resonance*" Wiley Inter science, New York (1972)
7. J. Subramanian, in "*Porphyrins and metalloporphyrins*" Edited by K. M. Smith (Elsevier, Amsterdam, 1975), p555
8. K. M. Smith, in "*Porphyrin and Metalloporphyrins*", Edited by K. M. Smith(Elsevier, Amsterdam, 1975) p3

9. J. Fajer, D. C. Borg, A. Forman, D. Dolphin and R. H. Felton., *J. Am. Chem. Soc.*, **92**, 3451 (1970)

10. J. H. Fuhrhop and D.Mauzerall., *J. Am. Chem. Soc.*, **90**, 3875 (1968)

11. R. H. Felton, D. Dolphin, D. C. Borg and J. Fajer., *J. Am. Chem. Soc.*, **91,** 196 (1969)

12. R. H. Felton, in *Porphyrins,* Edited by D. Dolphin (Acad.Press. NY, 1978) **Vol.III,** Chap.1

13. .M. Gouterman, in *Porphyrins,* Edited by D. Dolphin (Acad.Press. NY, 1978) **Vol.III,** Chap.1

14. G. E. Selyutin, A. A. Shklyaev,and V. F. Anerfrienko., *Dokl.Akad.Nauk.SSR.,* **255 (2),** 390 (1980)

15. M. Hoshino, S. Konishi, M. Imamura, S. Watanable, and Y. Hana., *Chem. Phys. lett.,* **102,** 259 (1983)

16. A. Tomba Singh and A.Lemtur, *Spec.Chim.Acta. Part.A .,* **59**, 1549 (2003)

17. J. Fajer, D. C. Borg, A. Forman, D. Dolphin, R. H. Felton, *J. Am. Chem. Soc* **92**, 3451 (1970)

18. E. T. Shimomura, M. A. Phillipi, M. M. Goff, W. F. Schuls and C. A. Reed., *J. Am. Chem. Soc.*, **103**, 6778 (1981)

19. A. S. Hinman, B. J. Pavelick, K. McGarty, *Can. J. Chem.*, **66,** 1589 (1988)

20. A. Bettelhein, B. A. White, S. A. Raybuck and R. W. Murray., *Inorg .Chem.*, **26,** 1009 (1987)

Appendix A

It has been observed that most of the substituted VOTPP systems undergo oxidation in the similar pattern to that of the VOTPP. In our ESR studies of the oxidation of VO[T(*o*-NO_2)PP] , VO[T(2,5-(OCH_3)$_2$)PP] , **VO[TpyP] and VO[T(*p*-OH)PP]** at room temperature we observe similar pattern[1]. Although we could not do low temperature measurements, we assume that these compounds give triplet state on oxidation with $SbCl_5$. A triplet state ESR spectrum of substituted Vanadyl porphyrin comes from its monomeric radical cation. The spin Hamiltonian for such a system is described elsewhere[1,2]. Diagonalisation of the Hamiltonian was done considering the system to be of axial symmetry. The powder spectrum is obtained by averaging over all angular orientations using Gaussian quadrature method. The value of A and D were adjusted to match the experimental spectrum. The parameter D is obtained from the spectrum considering the inter-electron vector parallel to the plane of the ring and normal to the 4-fold axis of the molecule. The D and g tensors are obtained in the principal axis parallel to the 4-fold symmetry axis. For axially symmetric system (considering Zeeman and zero field interaction only):

$$D_{x'x'} = D_{y'y'} = (D_{z'z'}/\ 2)\text{------------------------------}(\mathrm{A1})$$

$$D_{\parallel} = D_{x'x'} = D_{y'y'} = -D_{z'z'}$$

$$D_{z'z'}\ (\mathrm{IN\ MHz}) = 1.298 \times 10^4(\ g^2/R^3)\ \text{----------------}\ (\mathrm{A2})$$

Where R is in angstrom

And $g^2 = g^2 ll + 0.5\ g^2$

Here we consider only the dipolar interaction as the only factor contributing to the entire zero field splitting(ZFS). Thus, we obtained the inter electronic distances.

In the present case the inter electron distances were calculated using the soft ware Gaussian 2003.

References

1. A.Tomba singh, A.Lemtur, *Spectrochemica acta part A*, **59**, 1549 (2003)
2. J.Subramanian, V.P.shedbalkar, A.Lemtur, R.Chakaborty, T.N.Saloi, *J.Phys.chem.* **100**, 4770(1996)